**Department of Electronics and Electrical Communication Engineering.**

**Faculty of Engineering Cairo university**

# 2-element slot-fed microstrip patch antenna array

## Antenna and waveguides
## ELC 3050 – Fall 2024



| Student Name | ID | Sec | BN |
|---|---|---|---|
| بلال رمضان حلمي صميدة | 9220205 | 1 | 38 |
| عبدالرحمن محمد صلاح الدين ابو هندي | 9220473 | 2 | 39 |
| محمد عصام عبدالعظيم ابراهيم | 9220720 | 3 | 31 |
| محمود عبدالسلام عبدالصادق عبدالفتاح | 9220785 | 3 | 38 |
| نور اشرف احمد ماهر | 9220917 | 4 | 21 |
| يارا اسامة مهتدى ادريس | 9220954 | 4 | 26 |

**Under the supervision of:**
**Dr. Islam A. Eshrah**

# Table of Contents

# Table of Figures

# 1. Abstract

This report presents the design and analysis of two slot-fed microstrip patch 2 element antenna arrays, optimized for operation at **26 GHz**. Both designs were evaluated based on key parameters including gain, bandwidth, radiation efficiency, and return loss. The first design achieved a gain of **6.9 dB** and a radiation efficiency of **95%**. The second design outperformed the first with a higher gain of **9.16 dB** and a slightly lower radiation efficiency of **92%**. Both achieved the same operating bandwidth of **3.5 GHz** and **13.46%** as a relative operating bandwidth. The return loss for the first design was **-17.65 dB**, while the second design achieved **-31.75 dB**, indicating superior impedance matching in the latter. An equivalent circuit model was developed for both designs to simulate the return loss, showing good alignment with the electromagnetic (EM) simulation results.

The study also explored the effects of the spacing between antenna array elements, focusing on gain, mutual coupling, and active return loss. The first design has improved performance in radiation efficiency, axial ratio and mutual coupling, while the second design has improved performance in terms of gain, front-to-back ratio and side-lobe level. The impact of element spacing on mutual coupling and active return loss was analyzed, revealing a gradual decrease in mutual coupling with increased spacing.

In conclusion, both antenna designs exhibit promising characteristics, with the second design offering superior performance in gain, bandwidth, and impedance matching. Future work will focus on further optimization of the designs to enhance their performance for specific applications in communication systems.

# 2. Introduction and Problem description

## 2.1. Introduction

Microstrip Patch Antennas (MPAs) are pivotal in modern wireless communication systems due to their numerous advantages, including their low-profile design, lightweight construction, and seamless integration with other electronic components. These features make MPAs ideal for applications in high-frequency communication systems, such as 5G and millimeter-wave (mm-Wave) communications, where both bandwidth and performance are of paramount importance.

An MPA typically comprises a conducting patch, a dielectric substrate, and a ground plane. The conducting patch serves as the radiating element, while the ground plane provides a reflective surface to enhance radiation. The dielectric substrate separates the patch and the ground plane, influencing the antenna’s performance characteristics, including its bandwidth, efficiency, and radiation pattern. The geometry of the patch—commonly rectangular, circular, or other tailored shapes—is critical in determining the resonance frequency and overall antenna performance.

The design of an MPA involves careful selection of the substrate material, patch shape, and dimensions to satisfy specific resonance conditions. These parameters directly impact the antenna's ability to radiate efficiently at the desired frequency.

The increasing demand for high-speed and high-capacity wireless communication has driven the adoption of higher frequency bands, such as 5G and mm-Wave, which offer substantial bandwidth and low latency. However, operating at these high frequencies introduces challenges, including increased path loss and the need for precise beamforming to maintain signal quality. MPAs address these challenges effectively due to their inherent characteristics, such as:

- **Compact Design**: Their small size allows for integration into densely packed electronic systems without compromising performance.

- **High Gain and Directivity**: Essential for overcoming the propagation losses inherent in mm-Wave frequencies.
- **Scalability**: MPAs can be easily scaled into arrays to further enhance performance, such as gain and beam steering capabilities.
- **Ease of Fabrication**: Their planar structure enables mass production using standard PCB manufacturing techniques.

This report focuses on the design and implementation of a two-element array of slot-fed microstrip patch antennas operating at a frequency of 26 GHz. This frequency lies within the spectrum allocated for 5G and future wireless communication systems, making it a key enabler of next-generation connectivity.

The array configuration aims to address two critical aspects of high-frequency antenna design:

- **Improved Gain**: A single MPA, while efficient, may not provide the gain required for long-distance or high-performance applications. By combining two elements into an array, the gain can be significantly enhanced, making the antenna suitable for demanding environments.
- **Enhanced Directivity**: Precise control of the radiation pattern is essential in mm-Wave communications to mitigate interference and maximize signal reception. The two-element array allows for better directivity and beam steering, ensuring efficient utilization of the frequency spectrum.[1]

## 2.2. Problem description

The goal of this project is to design and analyze a two-element array of slot-fed microstrip patch antennas operating at 26 GHz. The primary objective is to achieve the desired radiation characteristics, including a specific gain, directivity, and impedance matching, while also addressing the challenges associated with high-frequency operation.

Key aspects of the project include:

1. **Antenna Design**: Design of individual slot-fed microstrip patch antennas, including the selection of patch shape, size, and dielectric material to ensure resonance at 26 GHz.
2. **Slot Feeding**: The use of slot feeding for the antenna, where the excitation is achieved through a slot in the ground plane. This method offers benefits such as reduced spurious radiation and better impedance matching but bad front-to-back ratio.
3. **Array Configuration**: The two-element array configuration must be designed to achieve constructive interference, enhancing the antenna's gain and directivity. The array elements must be spaced appropriately to prevent undesirable interference, mutual coupling or side lobes.
4. **Impedance Matching**: Ensuring that the antenna's impedance is matched to the transmission line and the input source to maximize power transfer and minimize reflections at the operating frequency of 26 GHz.
5. **Simulation and Optimization**: Using simulation software (such as CST Microwave Studio, HFSS, or others) to model the antenna array, simulate its performance, and optimize its design for optimal radiation characteristics.
6. **Performance Analysis**: Evaluating the antenna array's performance based on parameters such as return loss, gain, radiation pattern, and bandwidth to ensure that it meets the specifications for 26 GHz operation.

The challenge involves not only designing the antenna itself but also considering the effects of the operating frequency, material properties, array configuration, and the feeding network on overall performance. Additionally, challenges such as minimizing loss, optimizing the array layout, and managing mutual coupling between elements must be addressed.

By successfully designing this two-element array of slot-fed microstrip patch antennas, the project aims to by successfully designing this two-element array of slot-fed microstrip patch antennas, the project seeks to address the growing demand for compact, high-performance antennas that can operate efficiently in high-frequency bands. These antennas are integral to next-generation communication systems, such as 5G and beyond, where high data rates, low latency, and enhanced connectivity are critical. The use of a slot-fed configuration ensures improved impedance matching, reduced losses, and enhanced radiation efficiency, making the design suitable for applications requiring robust and reliable performance. Furthermore, this project aims to contribute to the advancement of antenna technology by providing a scalable and versatile solution that can be adapted for various emerging applications, including the Internet of Things (IoT), autonomous vehicles, and satellite communications, thereby supporting the evolution of modern communication infrastructure.[2]

# 3. Design Procedure

In this section, we will discuss the design procedure we followed to reach our final design. We actually worked on **two designs** in this project so we will discuss both of them, but we will divide the design procedure into two main stages, and each stage into multiple sections as follows:

1. **Single element slot-fed microstrip patch antenna.**
    A. Feeding structure
    B. Substrates material and thickness
    C. Slot dimensions
    D. Patch dimensions
2. **2-element array of the same antenna.**
    A. Feeding network
    B. Substrates and ground dimensions
    C. Elements spacing

## 3.1. Single element design

In this stage we worked on the single element alone before instantiating it in the full antenna system.

First, we will explain the feeding structure for **the slot-fed microstrip patch** antenna.

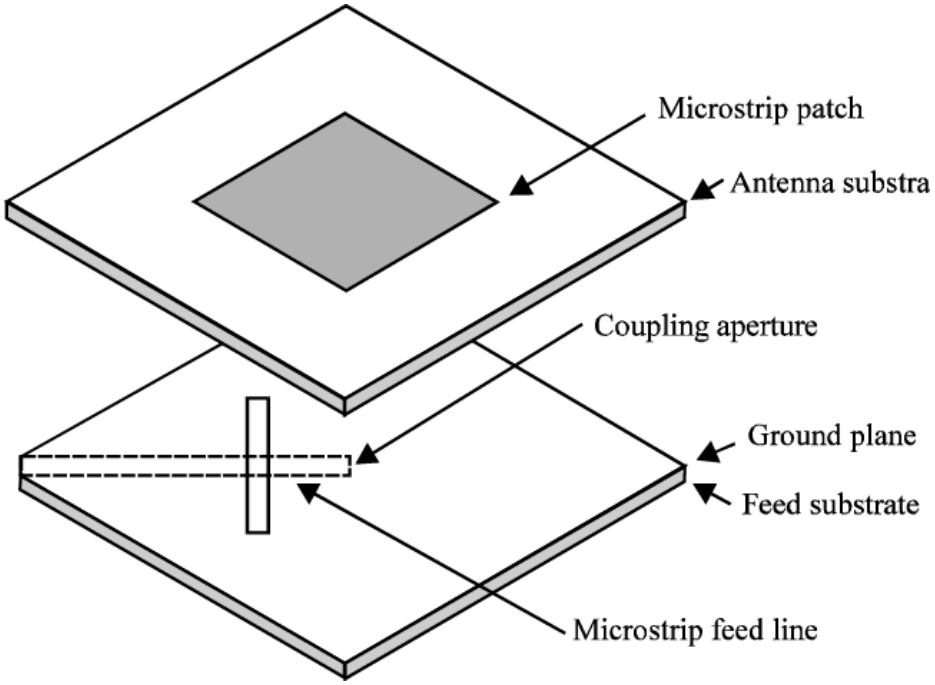


*Figure 1: Slot-fed microstrip patch antenna structure[5]*

## A. Feeding structure

The feeding structure is simply composed of microstrip feed line, feeding slot – which is known as coupling aperture – and the radiating microstrip patch in addition to two substrates: feed substrate and antenna substrate as illustrated in **figure 1**. The microstrip technology is simple, with just two different-shaped conductors and a substrate between them. So, we worked with the information we have, to initially build the single element structure. And that applies to both designs.

## B. Substrates material and thickness

For the substrates material we used **Rogers RO4350B**[3] with dielectric constant $\boldsymbol{DK(\epsilon_r) = 3.66}$ and loss tangent $\boldsymbol{tan\delta = 0.004}$ in the first design, and **Isola TerraGreen (R)** with dielectric constant $\boldsymbol{DK(\epsilon_r) = 3.44}$ and loss tangent $\boldsymbol{tan\delta = 0.0039}$ in the second design. The used materials dielectric constant is typically between 3 and 4, where in this range the dimensions and the cost are acceptable as there is a trade-off between them in choosing material, as $DK$ increases the dimensions decreases and the cost increases. We used the same material for both feed and antenna substrates.

For the substrates thickness, in the first design we chose $\boldsymbol{h_{feed\ substrate} = 0.508\ mm}$ from Rogers RO4350B standard thickness[3] to make it irradiative $(h < \lambda/10)$, and $\boldsymbol{h_{antenna\ substrate} = 0.78\ mm}$ to make it radiative $(h > \lambda/8)$.

In the second design we got the substrates thicknesses from designed paper with same DK material used in [4], $\boldsymbol{h_{feed\ substrate} = 0.1\ mm}$ and $\boldsymbol{h_{antenna\ substrate} = 0.8\ mm}$.

## C. Slots dimensions

For the slot dimensions, in the first design we got its dimensions from [1] matched with 50 Ω as a starting point before tuning. $\boldsymbol{L_{slot} = 0.3\ mm}$ and $\boldsymbol{W_{slot} = 2.4\ mm}$.

For the second design we got its dimensions from [4] matched with 50 Ω. $\boldsymbol{L_{slot}}$ **=0.15 mm** and $\boldsymbol{W_{slot}}$ **= 2.091 mm**.

### D. Patch dimensions

For the patch dimensions, in the first design we used an online calculator to make it operate at the required frequency 26 GHz with 50 Ω to be matched with typical sources and we did the same for the microstrip feed line then we tuned the patch length to get the desired resonating frequency – where theoretically $f_r = \frac{c}{2L\sqrt{\epsilon_r}}$ but it doesn't apply accurately so we used the online calculator – and tuned its width to get the desired input impedance 50 Ω. And finally, we got $\boldsymbol{W_{feed}}$ **= 1.11 mm**,
$\boldsymbol{L_{patch}}$ **= 1.96 mm** and $\boldsymbol{W_{patch}}$ **= 3.9 mm**.

In the second design we tested [4] dimensions, and tuned them to the following dimensions,
$\boldsymbol{W_{feed}}$ **= 0.22 mm** and $\boldsymbol{L_{patch}} = \boldsymbol{W_{patch}}$ **= 2.133 mm**.

Now, after we designed a single slot-fed microstrip patch antenna operating at 26 GHz with 50 Ω, we instantiated it to build a 2-element array, but it was not that easy. So, in the next section we will explain its design procedure.

## 3.2. 2-element array

### A. Feeding network

The feeding network in the first design is a T-splitter then two quarter-wave $(\lambda/4)$ sections, one in each branch and the lines impedance is as shown in **figure 2** to equally distribute the source power.

The second design is series fed and matched using one quarter-wave section as shown in **figure 3**. The space between the two antennas centers is a multiple of the wavelength $\lambda$ to make the two elements in phase.

We made sure that the matched terminations feeding network return loss is below -20 dB at the range of interest.

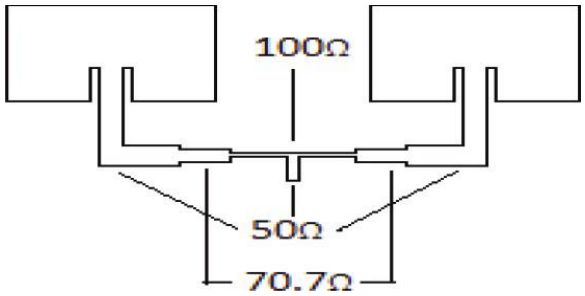


*Figure 2: First design Feeding network structure[6]*

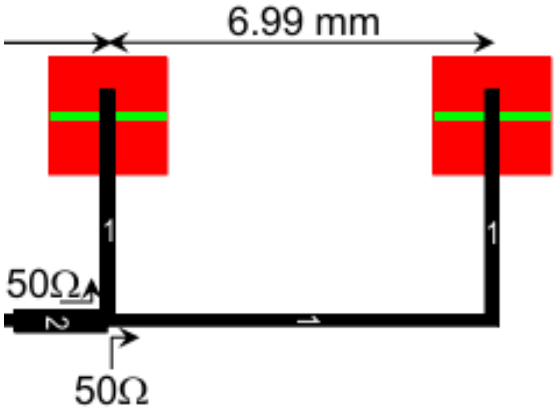


*Figure 3: Second design Feeding network structure[4]*

### B. Substrates and ground dimensions

The substrate and ground dimensions (area) influence the gain and radiation pattern, the gain is directly proportional to the area. We chose the dimensions to be **6 mmx35 mm** in the first design and **9 mmx20 mm** in the second design.

### C. Elements spacing

Elements spacing is a strong factor for the gain and radiation pattern. As the spacing increases the mutual coupling decreases but the feeding network losses increases, and at spacing higher than the wavelength $\lambda$ – in concern to the radiation pattern – two side lobes start to appear and attenuate the intended gain beam. After sweeping the spacing, we found that **10 mm** spacing is a sweet spot for the first design, while the spacing in the second design is **6.903 mm** such that the gain is optimum, no phase difference between the two elements and small side lobes in the first design while no side lobes in the second. It's discussed more in **section 4.8**.

# 4. Results and Discussion

## 4.1. Verification of EM tool results

Before discussing our results, we should verify the EM tool we used in the project. So, in this section we are willing to verify the EM tool results by benchmarking against another well-Known source. We designed a $\lambda/2$ dipole as shown in **figure 4** and observed the output if it's close to the excepted.

We used the material of the antenna (dipole) as copper and the radiation medium is air.

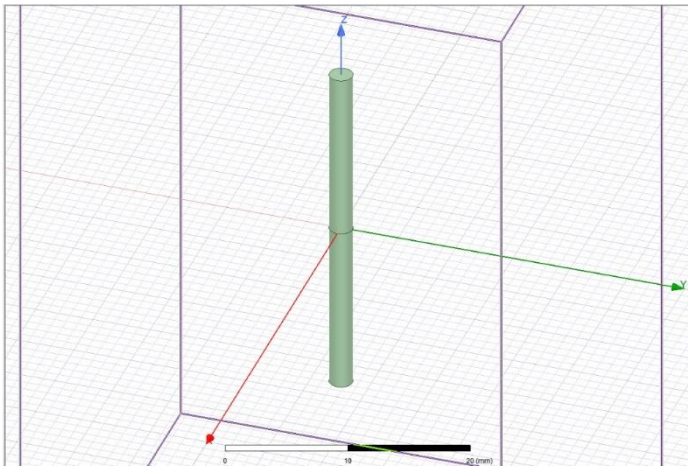

*Figure 4: $\lambda/2$ dipole structure*

In the first simulation we adjusted the diameter of the dipole to 1 mm and its length to 30 mm and the gap between the two wires – due to the supposed feeding – to 1 mm.

From the dipole length we will get the resonance frequency as follows:

$\frac{\lambda}{2} = 30 \rightarrow \lambda = 60$ mm, $\therefore f = \frac{c}{\lambda} = 5$ GHz.

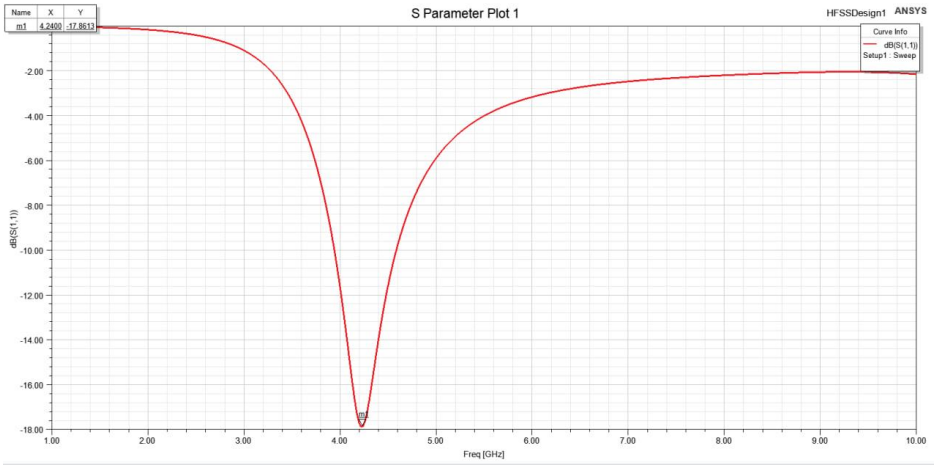


*Figure 5: $\lambda/2$ dipole return loss*

As we see in **figure 5**, it is resonant at **4.24 GHz** with **-17.86 dB** return loss far from the desired frequency as a result of the non-ideality due to the wire diameter and the gap between the two wires which are both ideally zero, so we reduced them to the minimum possible values for the current mesh size.

The parameters for the next simulation are $D_{dipole} = 0.01$ mm, $L_{dipole} = 30$ mm and the gap $= 0.01$ mm.

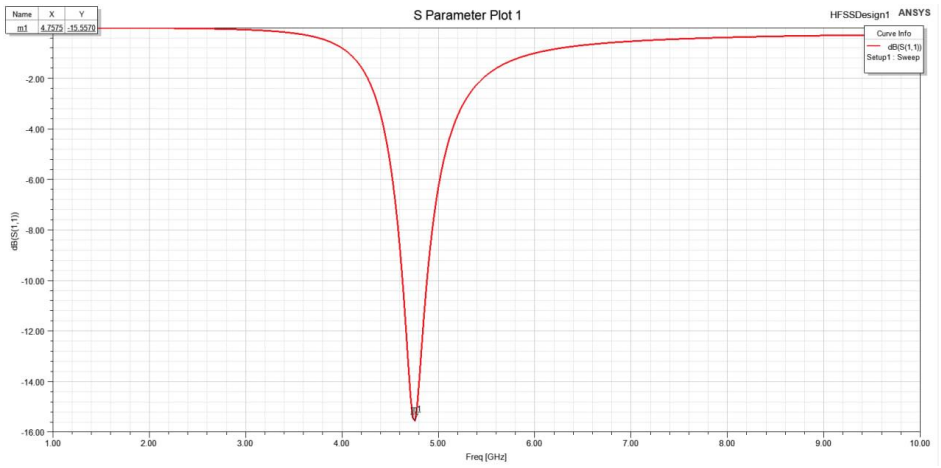


*Figure 6: New λ/2 dipole return loss (dB)*

As shown in **figure 6**, the frequency became **4.76 GHz** with **-15.56 dB** return loss closer to the ideal frequency.

For the radiation pattern, it is the same in both simulations and same as the expected shape from the lectures which is the donut shape and almost no gain in the dipole axis as shown in **figures 7-10**. But it's more directive with directivity **1.8** due to non-ideality as we discussed above and have the effect of magnetic current which we didn't dive into.

Note that the illustrated figure is the dipole gain but it's the same as the directivity because it's matched with the source.

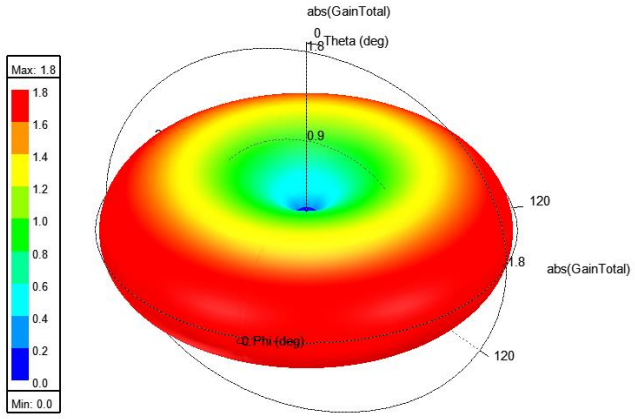


*Figure 8: λ/2 dipole 3D polar gain (linear)*

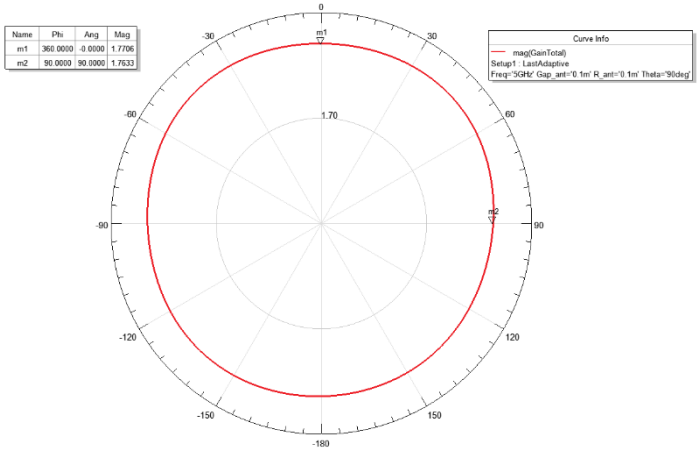


*Figure 7: λ/2 dipole Radiation pattern (dB) in H(xy)-plane*

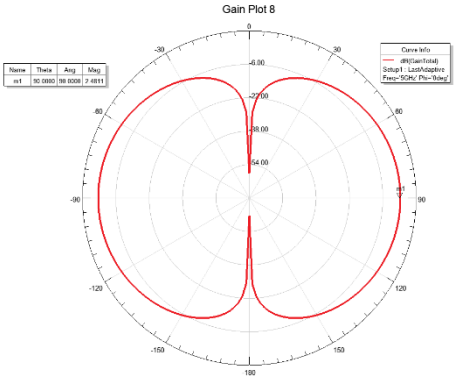


*Figure 9: λ/2 dipole Radiation pattern (dB) in the xz-plane*

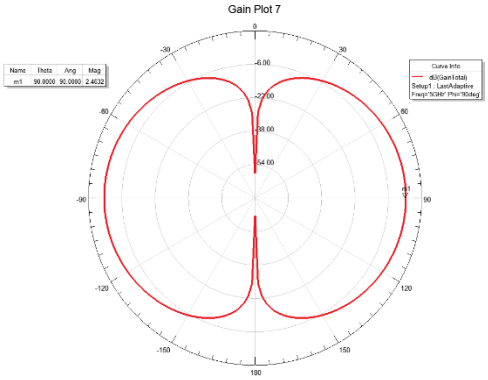


*Figure 10: λ/2 dipole Radiation pattern (dB) in the yz-plane*

## 4.2. Return loss

Now, after we verified our EM tool we will present and discuss our simulation results for both designs in this project starting with the return loss.

The return loss is a very important antenna parameter, as it provides critical insights into the performance of the antenna. Specifically, it indicates the level of matching between the antenna and the transmission line at the operating frequency. A well-matched antenna will exhibit a high return loss (typically a negative value, indicating low reflection), which is essential for efficient power transfer.

In addition to matching, the return loss also provides information about the matching bandwidth around the operating frequency. This bandwidth is the range of frequencies over which the antenna maintains acceptable matching (typically less than -10 or -12 dB).

### A. First design

By examining the return loss graphs for the first design in **figure 11**, we can tell that the first design has a return loss of **-17.65 dB** at 26 GHz and a matching bandwidth of **3.5 GHz (from 24.88 GHz to 28.38 GHz)**, i.e., **13.46%** relative matching BW.

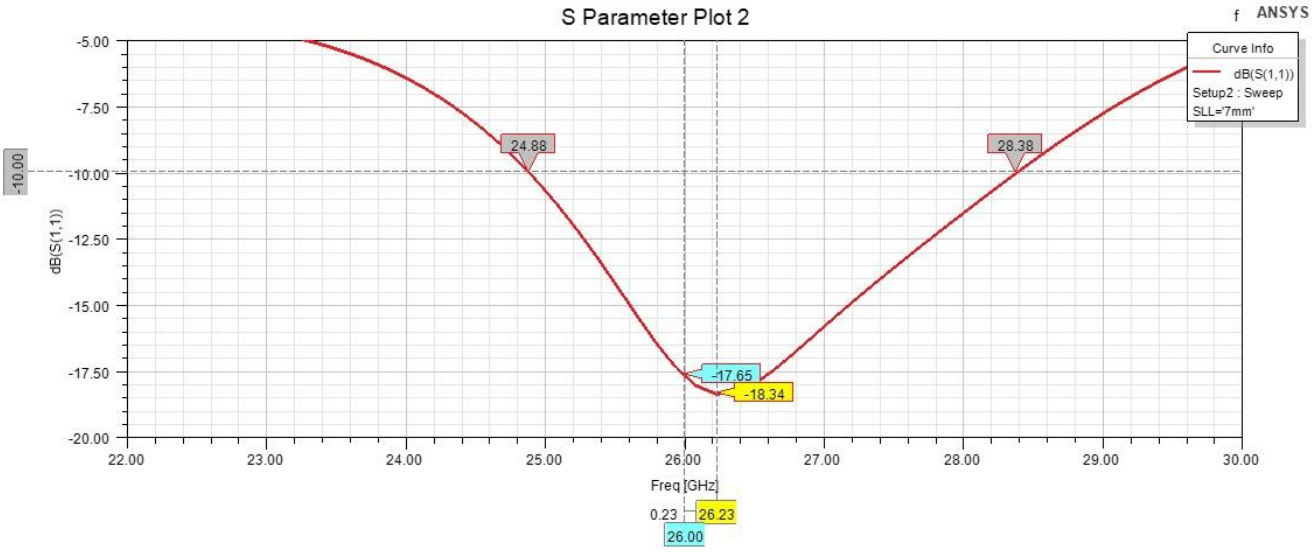


*Figure 11: First design Return loss (dB)*

## B. Second design

From **figure 12**, the second design has a return loss of **-31.75 dB** at 26 GHz and a matching bandwidth of **7.95 GHz (from 24.81 GHz to 32.76 GHz)**, i.e., **30.5%** relative matching BW.

Therefore, the second design has better return loss results, which indicates improved matching at the operating frequency and offers a wider return loss bandwidth.

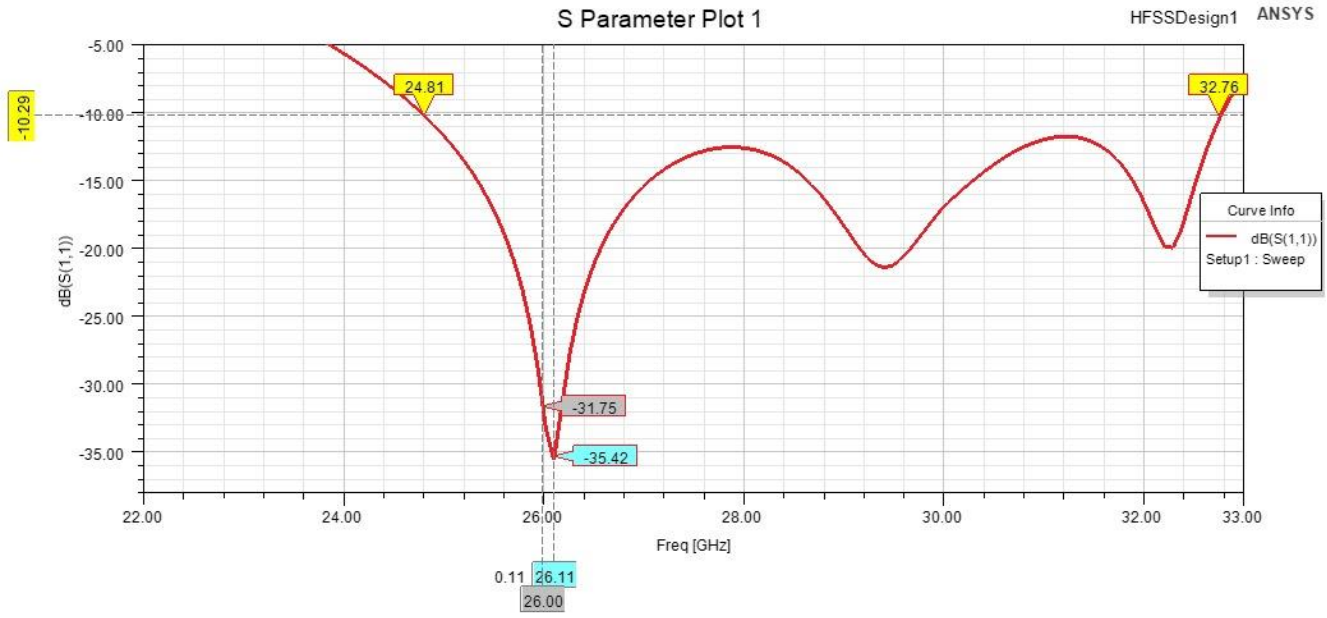


*Figure 12: Second design Return loss (dB)*

# 4.3. The input impedance of the designed antenna on the Smith chart

The input impedance of the two designs was analyzed using Ansys-HFSS Smith chart, focusing on their behavior at the target frequency of **26 GHz**. This analysis is crucial for ensuring efficient power transfer between the antenna and the feeding transmission line, minimizing reflections and achieving good impedance matching.

## A. First design:

The Smith Chart was used to visualize the impedance behavior across the frequency range of interest. At **26 GHz**, the normalized simulated input impedance $\boldsymbol{Z_{in_{normalized}}}$ was found to be approximately **1.267 – j0.14 Ω** from **figure 13**, by which we can get the input impedance by multiplying by 50. So, $\boldsymbol{Z_{in}}$ **= 63.35 – j7 Ω**, which is close to the target characteristic impedance of **50 Ω**. The input impedance's real and imaginary components indicate the antenna's resistive and reactive behavior, respectively. To minimize the reflection coefficient (S11), the reactive part was tuned to near-zero, ensuring resonance at the desired frequency. Impedance matching was verified through the calculated **reflection coefficient**, which showed a value of **Γ ≈ 0.1259** that was calculated from the got value of S11, confirming that most of the input power is radiated by the antenna.

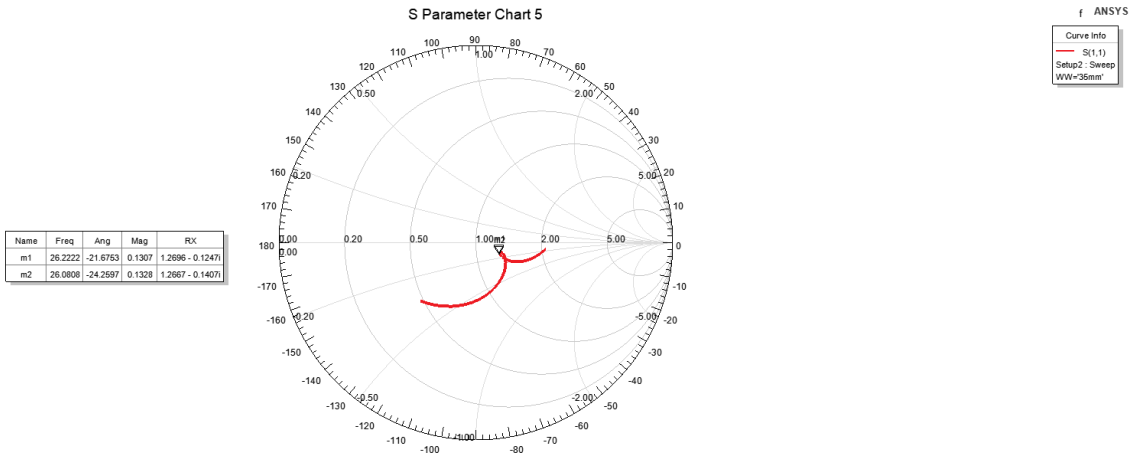


*Figure 13: Input impedance of first design on Smith chart*

## B. Second design:

The Smith Chart was used to visualize the impedance behavior across the frequency range of interest. At **26 GHz**, the normalized simulated input impedance $Z_{in_{normalized}}$ was found to be approximately **0.969 + j0.0338 Ω** from **figure 14**, by which we can get the input impedance by multiplying by 50. So, $Z_{in}$ **= 48.445 – j1.69 Ω**, which is close to the target characteristic impedance of **50 Ω**. The input impedance's real and imaginary components indicate the antenna's resistive and reactive behavior, respectively. To minimize the reflection coefficient (S11), the reactive part was tuned to near-zero, ensuring resonance at the desired frequency. Impedance matching was verified through the calculated **reflection coefficient**, which showed a value of **Γ ≈ 0.0259** that was calculated from the got value of S11, confirming that most of the input power is radiated by the antenna.

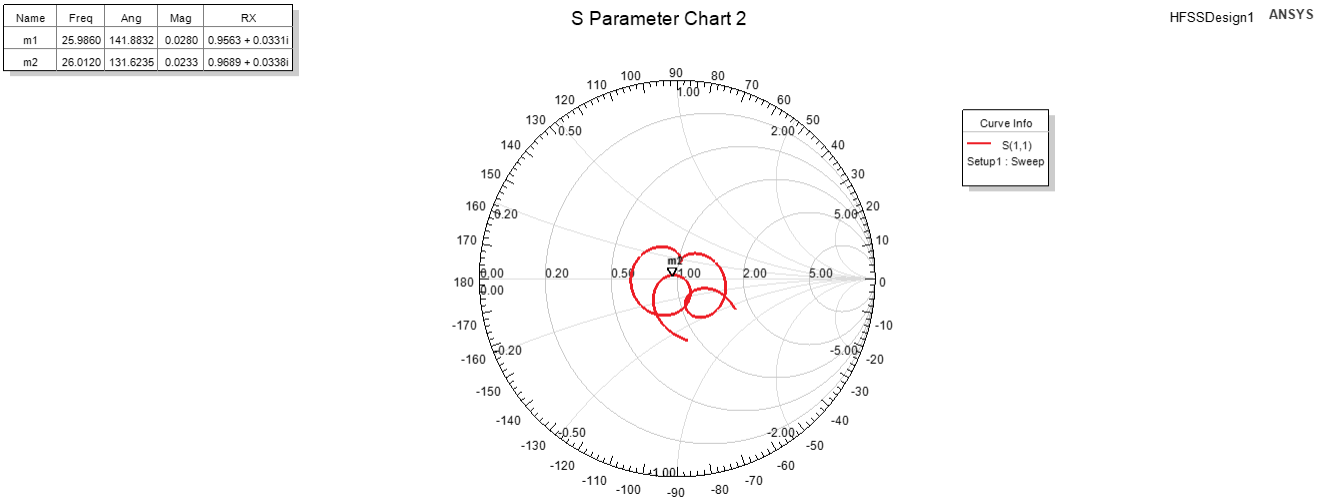


*Figure 14: Input impedance of second design on Smith chart*

# 4.4. The radiation pattern (co-pol and x-pol) in the E and H planes.

This analysis is essential for evaluating the azimuth and elevation beamwidths, gain in the intended direction, front-to-back ratio, the side-lobe level, the directional radiation characteristics, and polarization purity at the target frequency 26 GHz.

## A. First design:

In **figure 18**, we can see the gain of the antenna in dB in the main direction which is **6.9 dB**, and we can estimate the beamwidth from that graph about **96 degrees** in the xz-plane. The front-to-back ratio is around **6.25 dB**, that's because the slot-fed antennas have bad front to back ratio because of the gap in the ground. And we can see the same from **figure 17** in the yz-plane graph but only the difference in beamwidth in that direction, which is quite higher than **28 degrees**, smaller beamwidth is due to the presence of 2 antennas on y-axis, and we can get also the side-lobe level (SLL) which equals **8.5 dB**. In **figure 24**, the beamwidth in both planes appears more accurate and it equals **28.7 degrees** in yz-plane and **95 degrees** in xz-plane.

As shown in **figures 15 &16**, It can be observed that the first design achieves a large cross-polarization discrimination (XPD) of around **48 dB** in **figure 22**, show the axial ratio versus theta in two different planes and the mean value is about **53.69 dB**. **Figure 23** shows the axial ratio in the boresight for different frequencies, the axial ratio is above **30 dB** in the range of interest (the frequencies from 20 to 32 GHz).

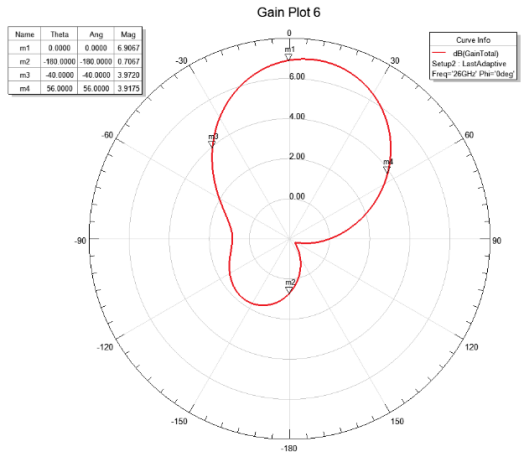


*Figure 18: First design Radiation pattern (dB) in the xz-plane*

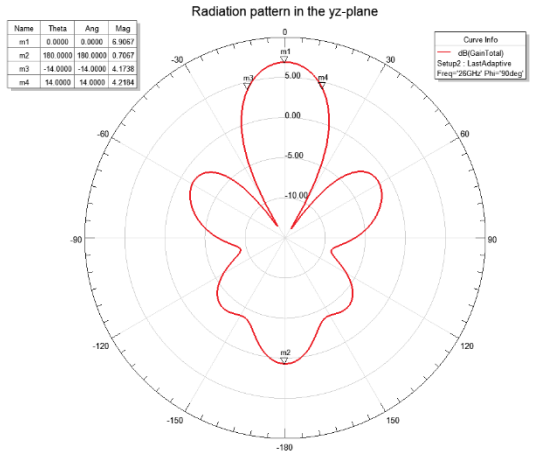


*Figure 17: First design Radiation pattern (dB) in the yz-plane*

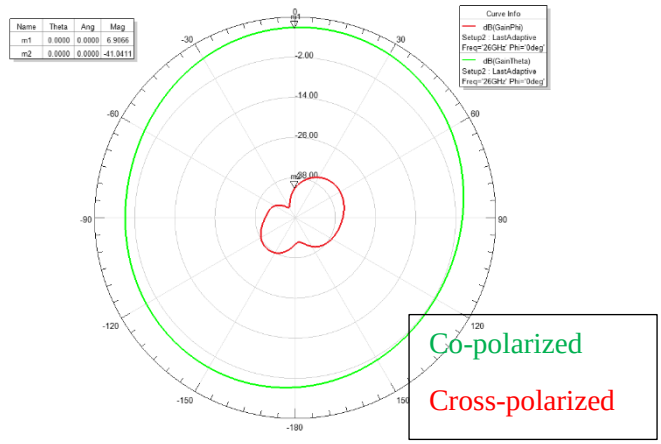


*Figure 15: First design Co & Cross Polarized Fields (dB) in H-Plane*

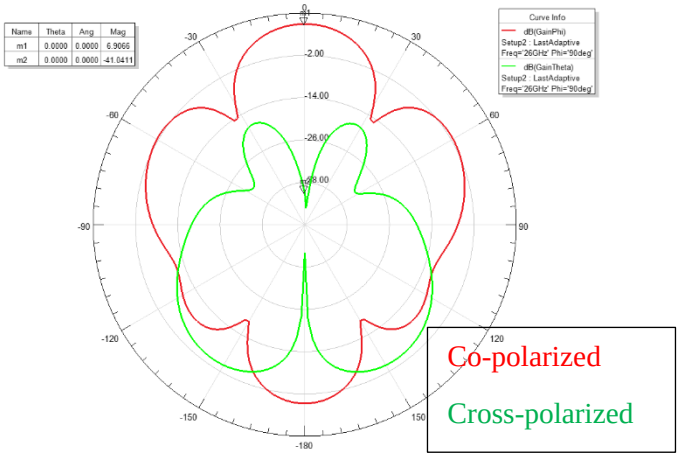


*Figure 16: First design Co & Cross Polarized Fields (dB) in E-Plane*

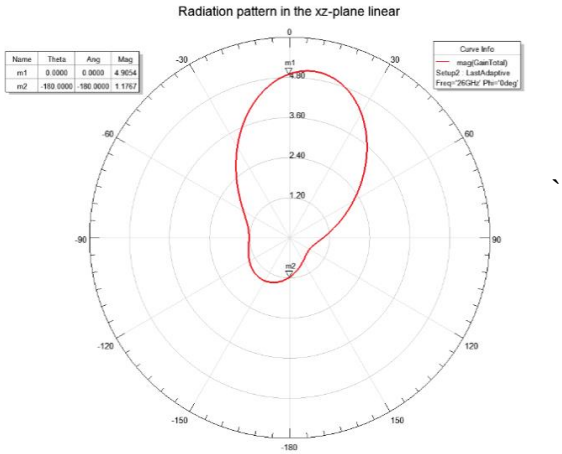


*Figure 20: First design Radiation pattern (linear) in the xz-plane*

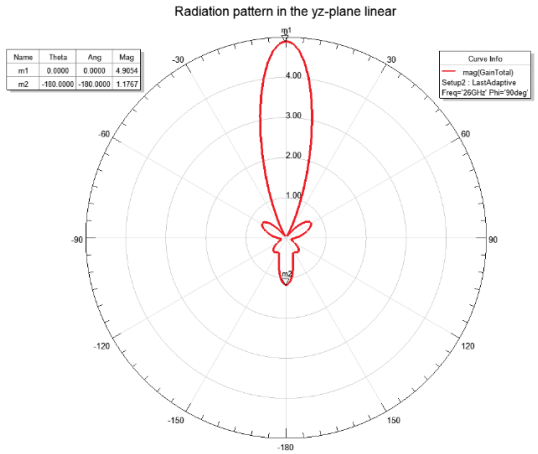


*Figure 19: First design Radiation pattern (linear) in the yz-plane*

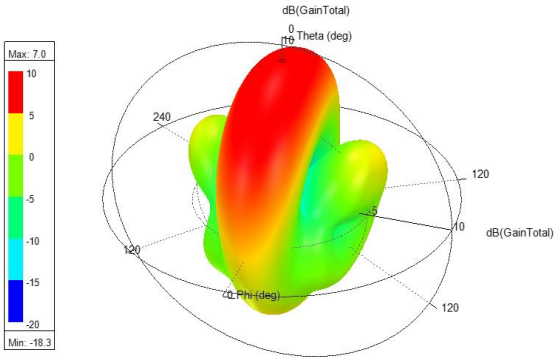


*Figure 21: First design 3D Polar Plot of Gain (dB)*

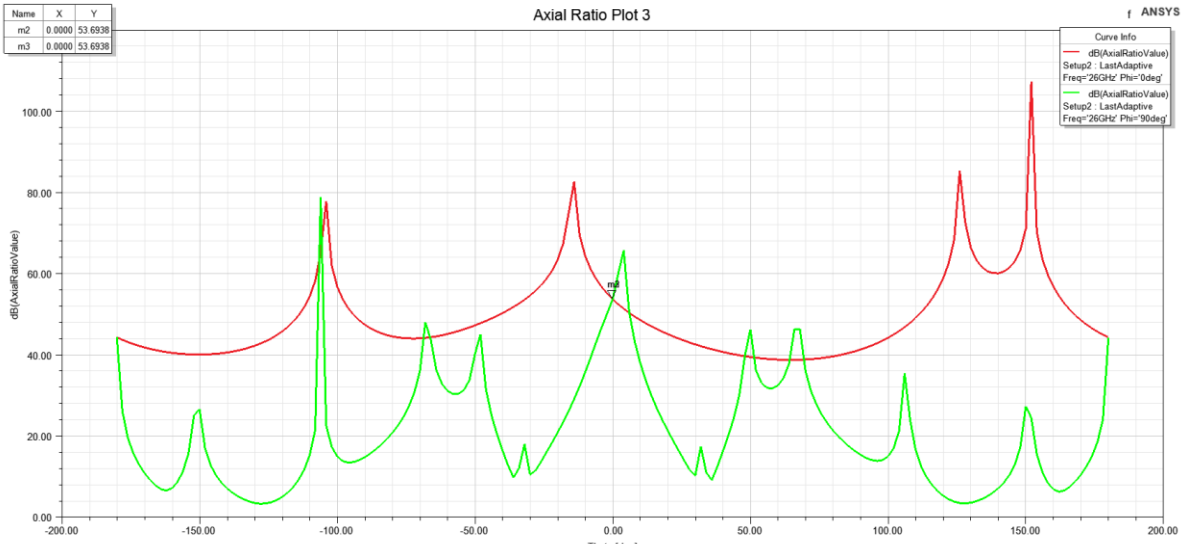


*Figure 22: First design Axial ratio (dB) vs theta*

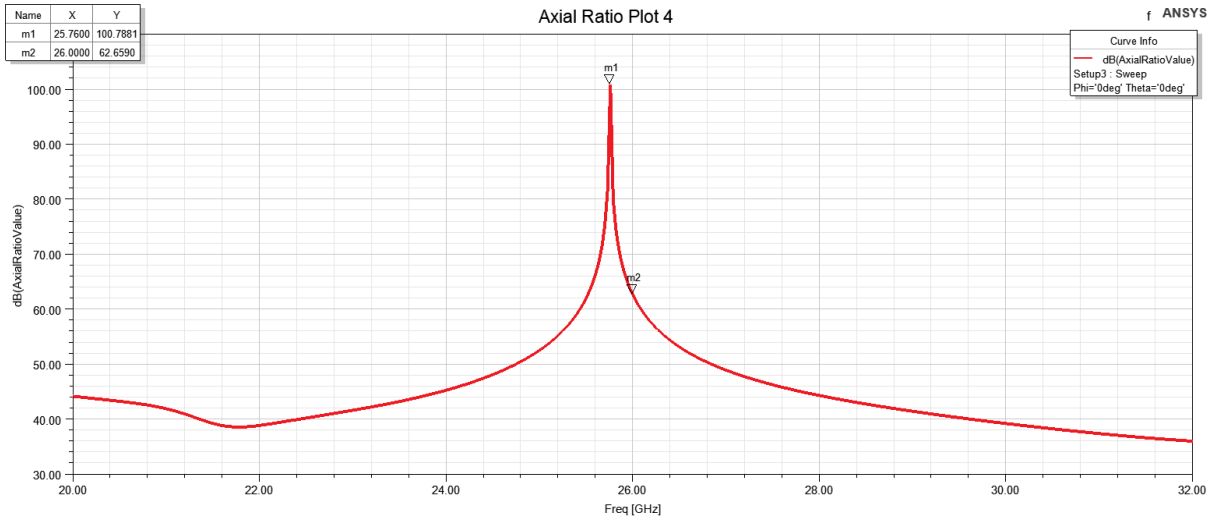


*Figure 23: First design axial ratio (dB) vs frequency*

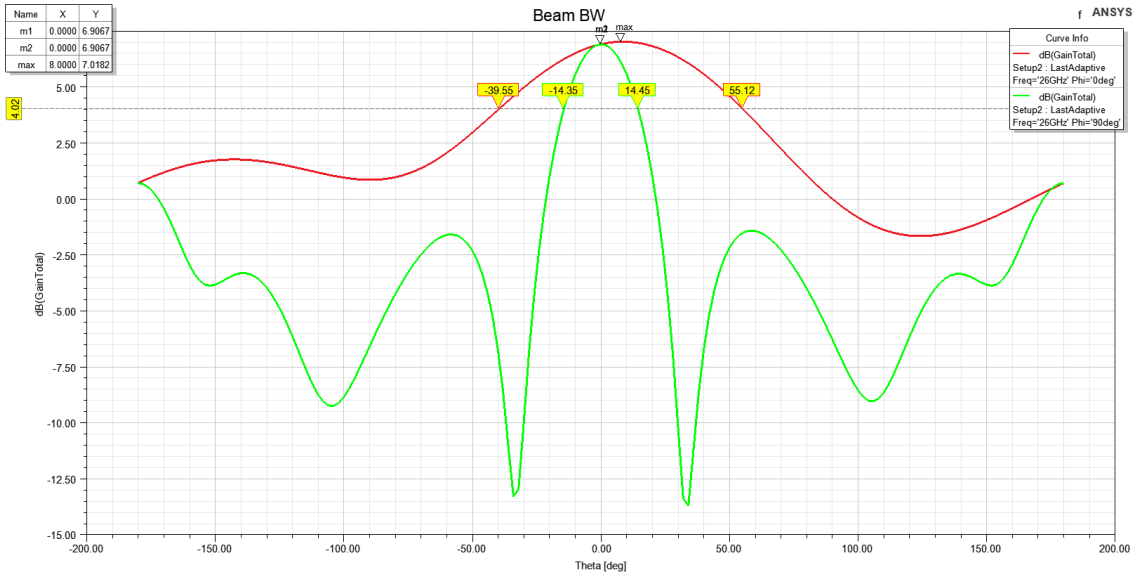


*Figure 24: First design Cartesian radiation patterns (dB)*

## B. Second design:

In **figure 27**, we can see the gain of the antenna in dB in the main direction which is **9.16 dB**. The front-to-back ratio is around **10.66 dB**, that's because the slot-fed antennas have bad front to back ratio because of the gap in the ground. In **figure 34**, the beamwidth in both planes appears more accurate and it equals **43.76 degrees** in yz-plane and **76 degrees** in xz-plane, smaller beamwidth in yz-plane is due to the presence of 2 antennas on y-axis, and the side-lobe level (SLL) equals **22 dB**.

As shown in **figures 25 &26**, It can be observed that the second design achieves a large cross-polarization discrimination (XPD) of around **36.84 dB** in **figure 32**, show the axial ratio versus theta in two different planes and the mean value is about **38.7 dB**. **Figure 33** shows the axial ratio in the boresight for different frequencies, the axial ratio is above **25 dB** in the range of interest (the frequencies from 20 to 32 GHz).

So, the first design has better axial ratio (cleaner linear polarization), but the second design has higher gain, front-to-back ratio and SLL. It's obvious in **figures 19, 20, 30 &31** that the second design has much better SLL.

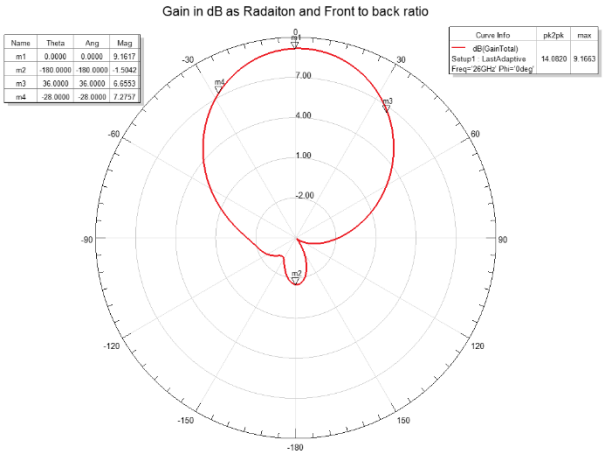


*Figure 27: Second design Radiation pattern (dB) in the xz-plane*

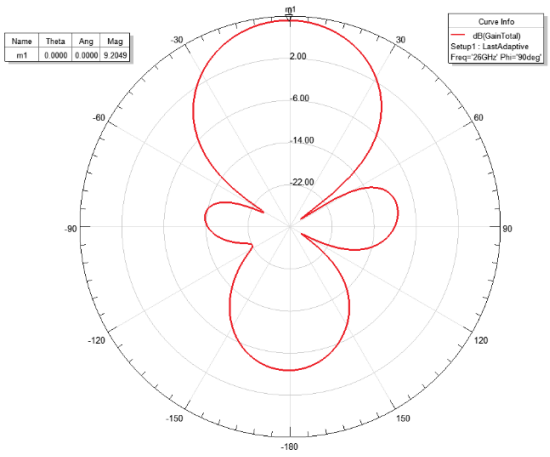


*Figure 28: Second design Radiation pattern (dB) in the yz-plane*

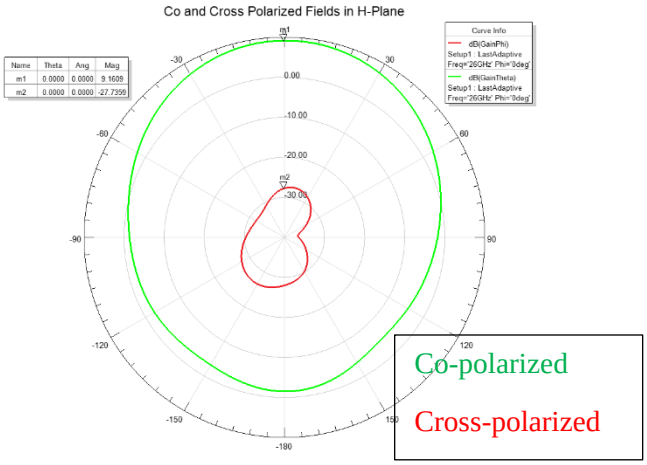


*Figure 26: Second design Co & Cross Polarized Fields (dB) in H-Plane*

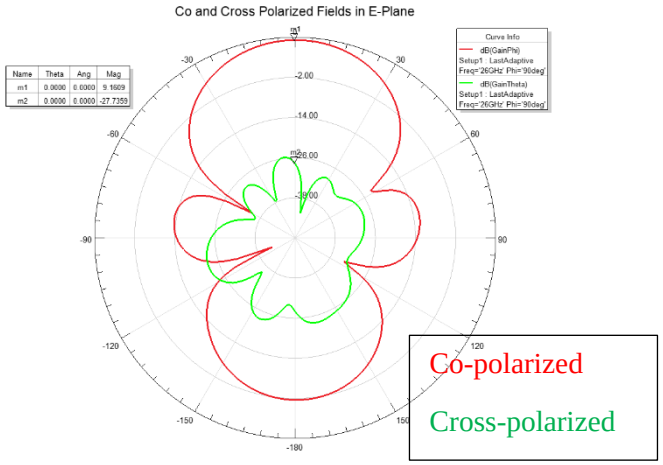


*Figure 25: Second design Co & Cross Polarized Fields (dB) in E-Plane*

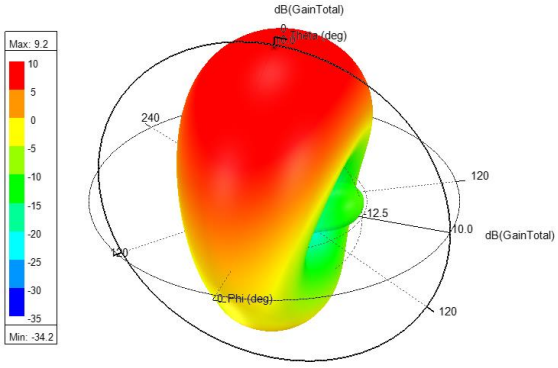


*Figure 29: Second design 3D Polar Plot of Gain (dB)*

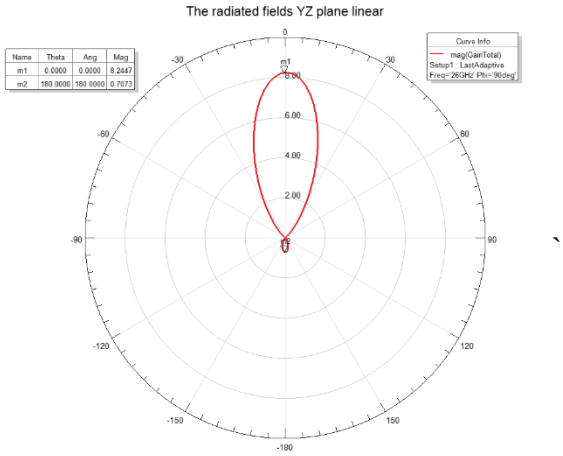


*Figure 30: Second design Radiation pattern (linear) in the xz-plane*

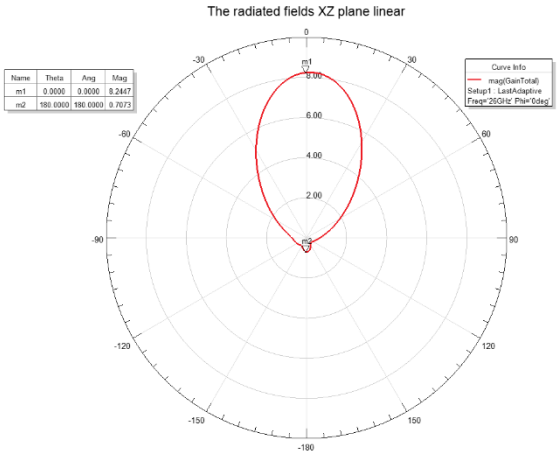


*Figure 31: Second design Radiation pattern (linear) in the yz-plane*

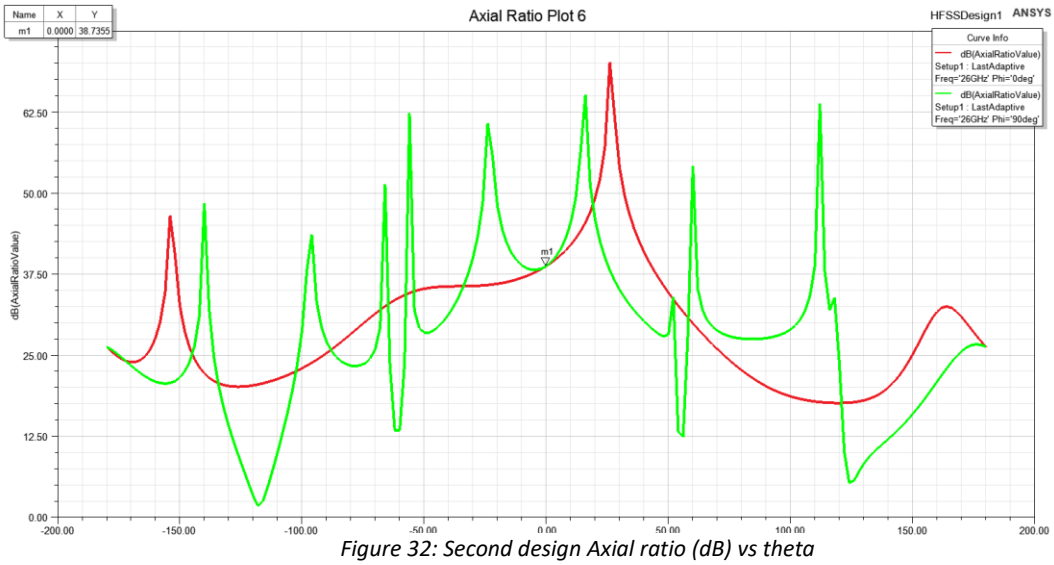


*Figure 32: Second design Axial ratio (dB) vs theta*

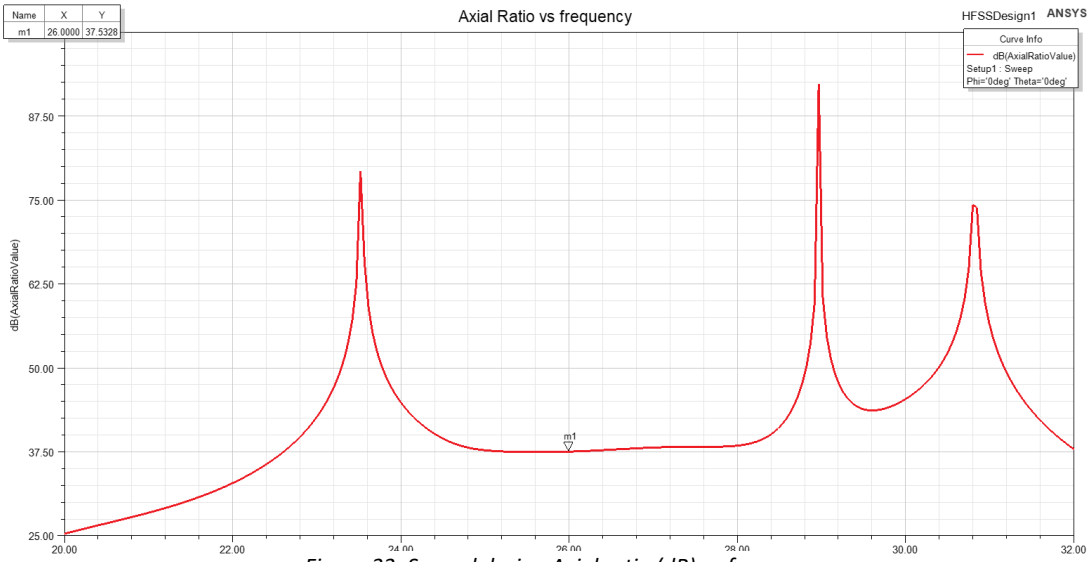


*Figure 33: Second design Axial ratio (dB) vs frequency*

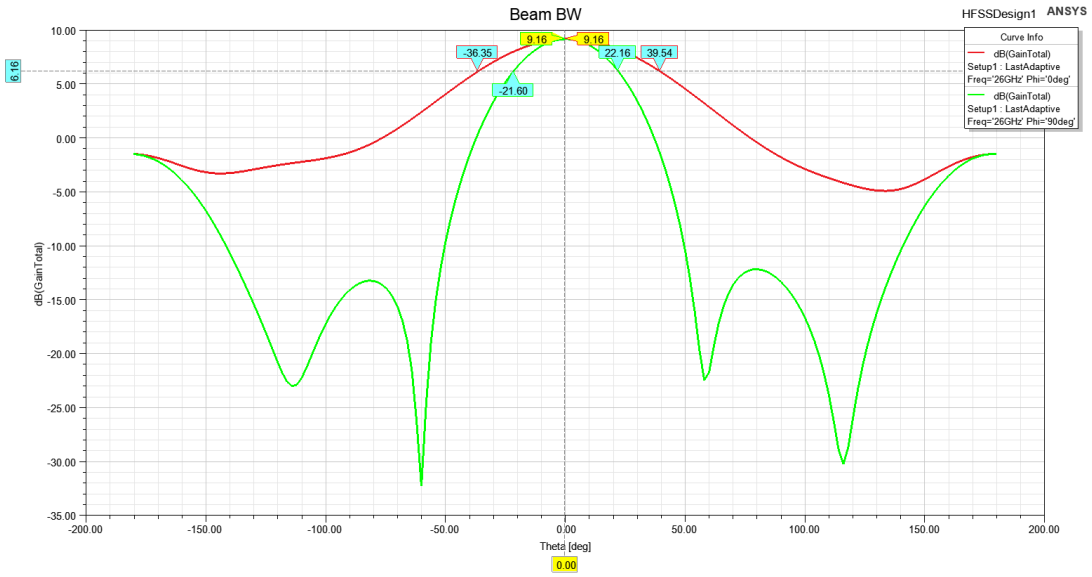


*Figure 34: Second design Cartesian radiation patterns (dB)*

# 4.5. The gain and radiation efficiency of the antenna vs frequency.

This results section is focused on estimating the intended-direction gain and radiation efficiency at the target frequency 26 GHz and the 1-dB gain bandwidth for the antenna array.

## A. First design:

As shown in **figures 35 &36**, the first design has a gain of **6.9 dB** at 26 GHz and radiation efficiency of **95%**. The 1-dB gain bandwidth is evaluated such that the cut-off values is less than the gain at 26 GHz by 1-dB, and it's hence the first design 1-dB gain bandwidth is **6 GHz (from 24.1 GHz to 30.1 GHz)**, i.e., **23%** relative 1-dB gain BW. We can observe the realized gain in **figure 37** to evaluate the operating bandwidth as a replacement for the 1-dB gain bandwidth and the matching bandwidth which is **4.1 GHz (from 24.7 GHz to 28.8 GHz)**, i.e., **15.76%** relative realized 1-dB gain bandwidth.

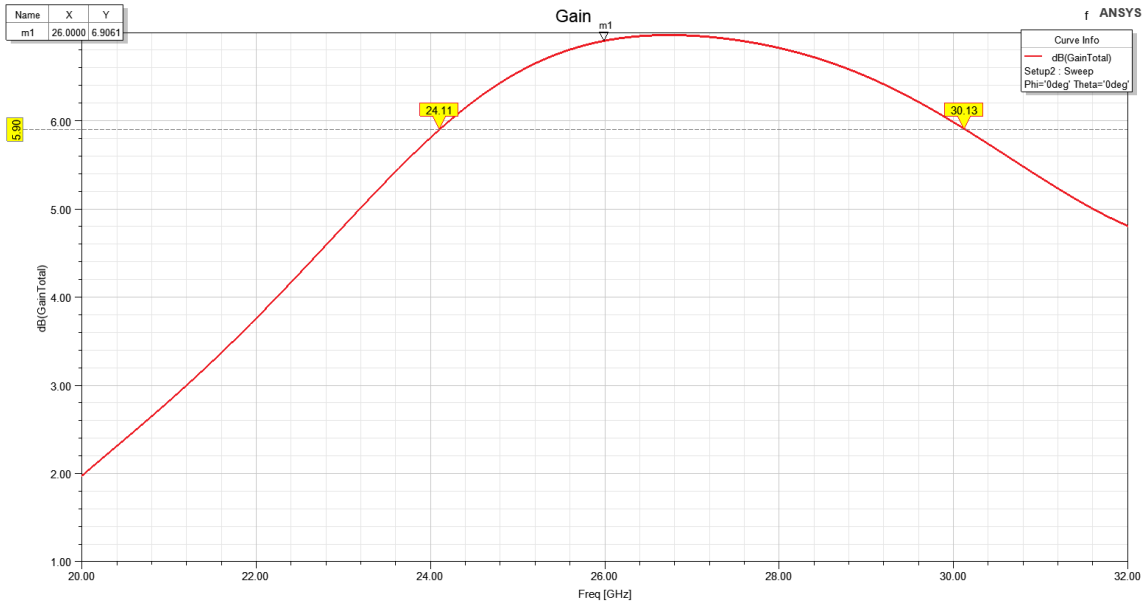


*Figure 35: First design Gain (dB) vs frequency*

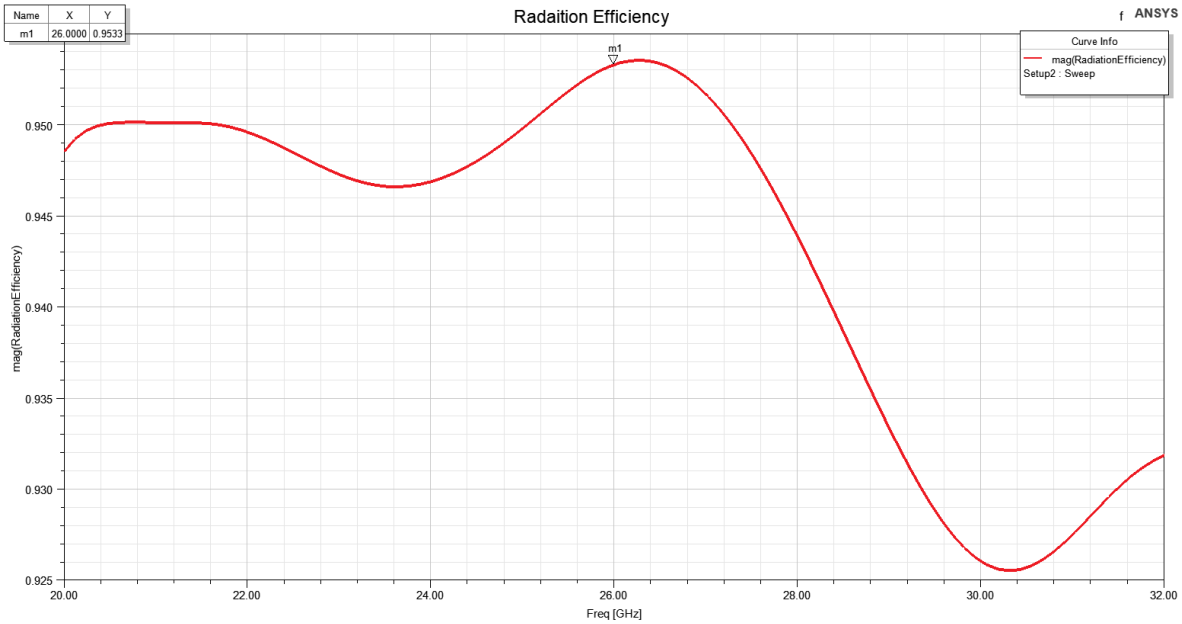


*Figure 36: First design Radiation efficiency (linear) vs frequency*

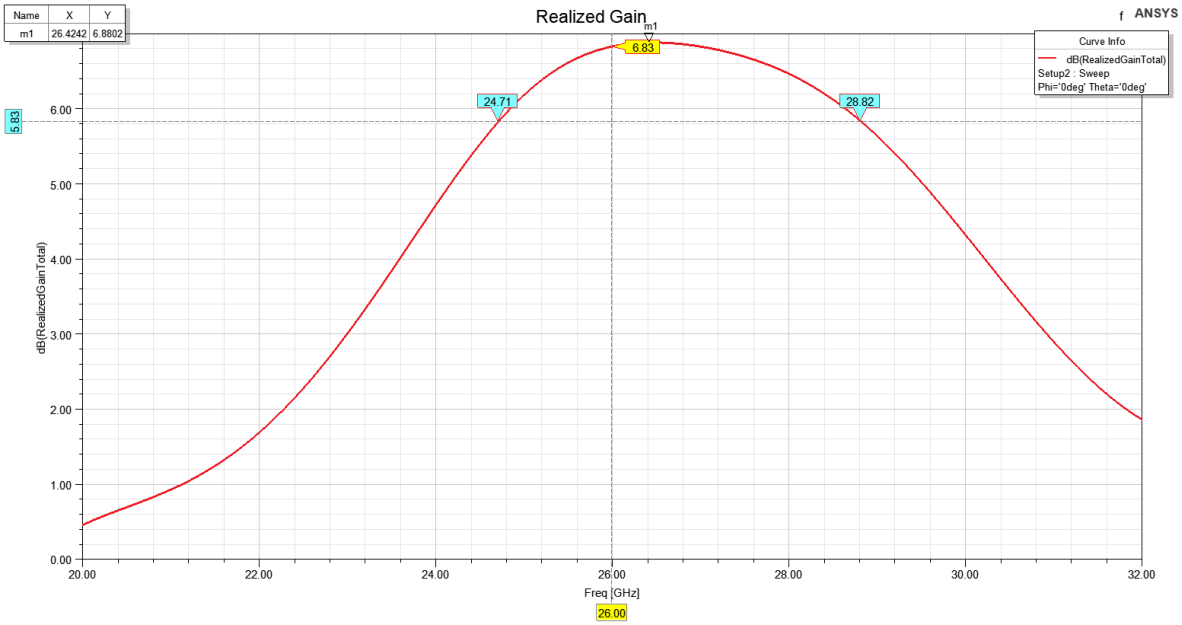


*Figure 37: First design Realized gain (dB) vs frequency*

## B. Second design:

As shown in **figures 38 &39**, the first design has a gain of **9.1 dB** at 26 GHz and radiation efficiency of **92%**. The 1-dB gain bandwidth is evaluated such that the cut-off values is less than the gain at 26 GHz by 1-dB, and it's hence the first design 1-dB gain bandwidth is **3.8 GHz (from 24.5 GHz to 28.3 GHz)**, i.e., **14.6%** relative 1-dB gain BW. We can observe the realized gain in **figure 40** to evaluate the operating bandwidth as a replacement for the 1-dB gain bandwidth and the matching bandwidth which is **3.3 GHz (from 24.9 GHz to 28.2 GHz)**, i.e., **12.7%** relative realized 1-dB gain bandwidth.

Hence, the first design has higher radiation efficiency, relative 1-dB gain and realized 1-dB gain bandwidths.

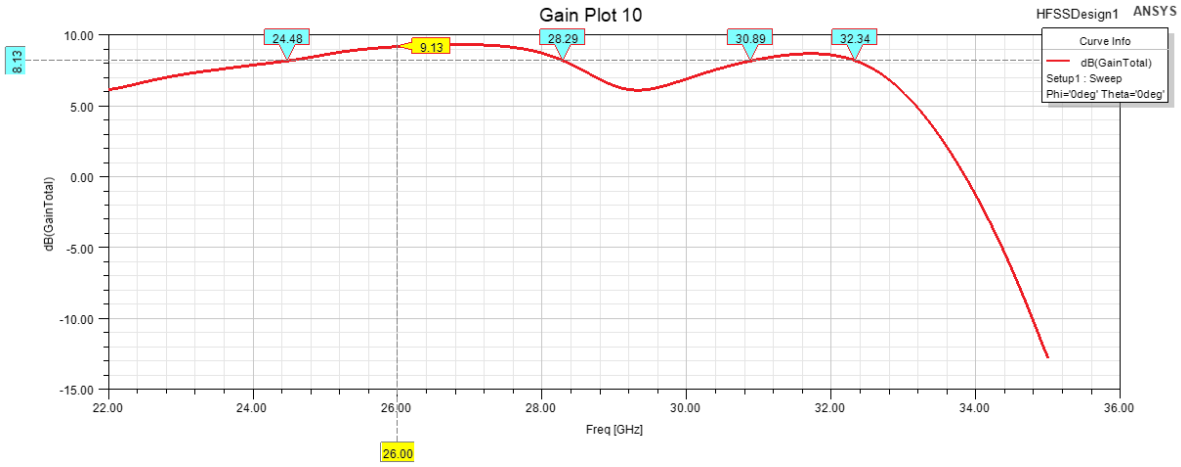


*Figure 38: Second design Gain (dB) vs frequency*

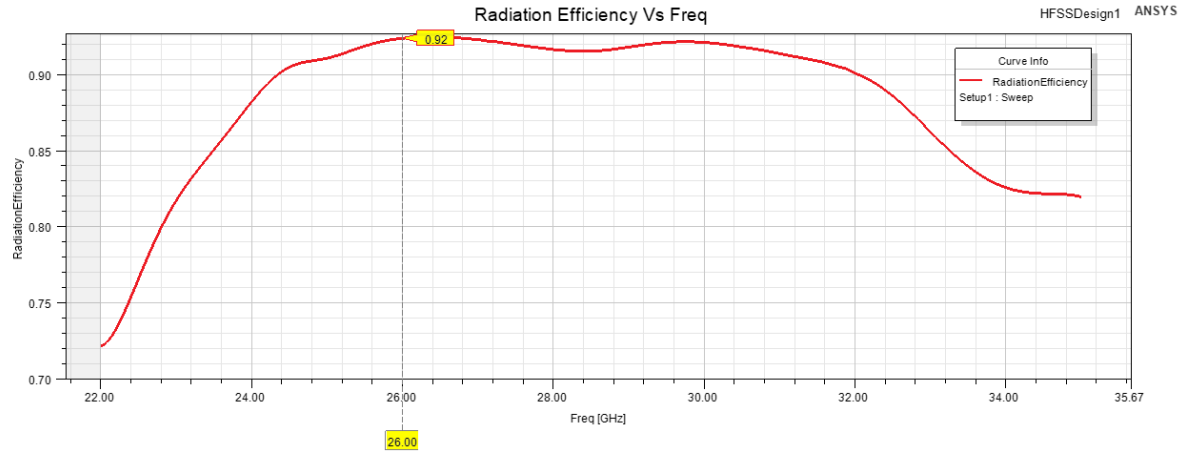


*Figure 39: Second design Radiation efficiency (linear) vs frequency*

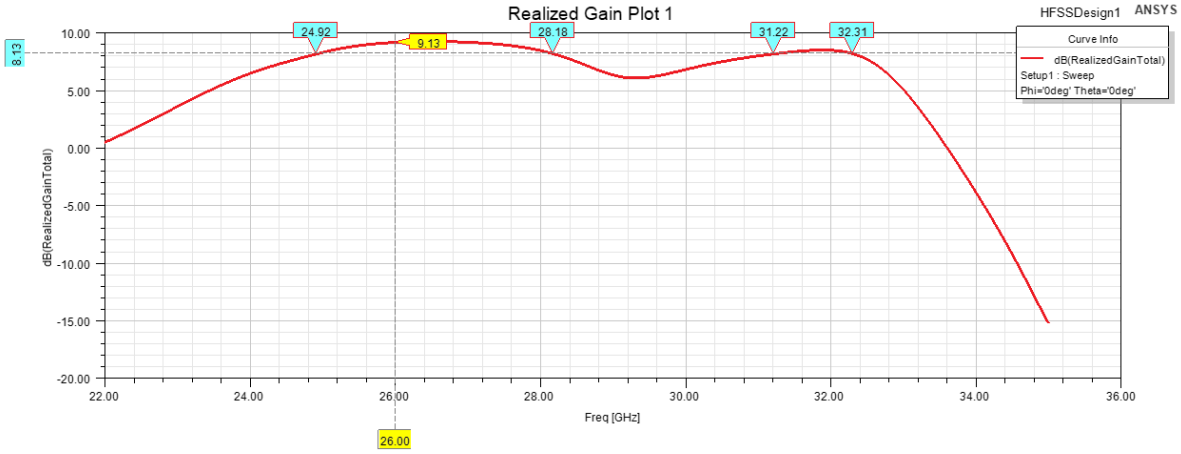


*Figure 40: Second design Realized gain (dB) vs frequency*

## 4.6. The more specific antenna characteristics

Rather than other feeding techniques, the slot-fed antennas have moderate bandwidth, high radiation efficiency and flexible polarization control, but at the cost of the front-to-back ratio due to the gap in the ground as mentioned in **section 4.4**.

### A. First design

As mentioned in **sections 4.2, 4.3** and **4.4**, the matching BW is from **24.88 GHz** to **28.38 GHz**, and the 1-dB gain BW is from**24.1 GHz** to **30.1 GHz**, so, the operating bandwidth is their intersection from **24.88 GHz** to **28.38 GHz (3.5 GHz)**, i.e., **13.46%** relative operating bandwidth, the radiation efficiency is **95%**, and the front-to-back ratio is just **6.25 dB**.

### B. Second design

As mentioned in **sections 4.2, 4.3** and **4.4**, the matching BW is from **24.8 GHz** to **32.76 GHz**, and the 1-dB gain BW is from **24.5 GHz** to **28.3 GHz**, so, the operating bandwidth is their intersection from **24.8 GHz** to **28.3 GHz (3.5 GHz)**, i.e., **13.46%** relative operating bandwidth, the radiation efficiency is **92%**, and the front-to-back ratio is just **10.66 dB**.

## 4.7. Equivalent circuit model of the antenna

To gain a deeper understanding of the slot-fed 2-element array antenna's impedance behavior at the target frequency of **26 GHz**, an equivalent circuit model for S11 was developed using **Advanced Design System (ADS)**. This model provides a simplified yet accurate representation of the antenna's electrical behavior and validates the EM simulation results.

The equivalent circuit was constructed in ADS using a combination of lumped elements, including resistors (R), inductors (L), and capacitors (C), to replicate the antenna's impedance characteristics. The built-in **optimization tool** in ADS was used to fine-tune the circuit parameters to achieve the best match with the return loss **(S11)** obtained from the EM simulations.

### A. First Design

We started the operation of getting the model by a few number of parameters but to get accurate results and easy use of the optimizer, we increased the number of parameters to get more degrees of freedom for the simulator to optimize. The equivalent circuit is shown in **figure 41**.

The reflection coefficient **(S11)** calculated from the optimized circuit model was overlaid with the EM simulation results, showing a high degree of alignment, particularly at **26 GHz** as shown in **figure 42**.

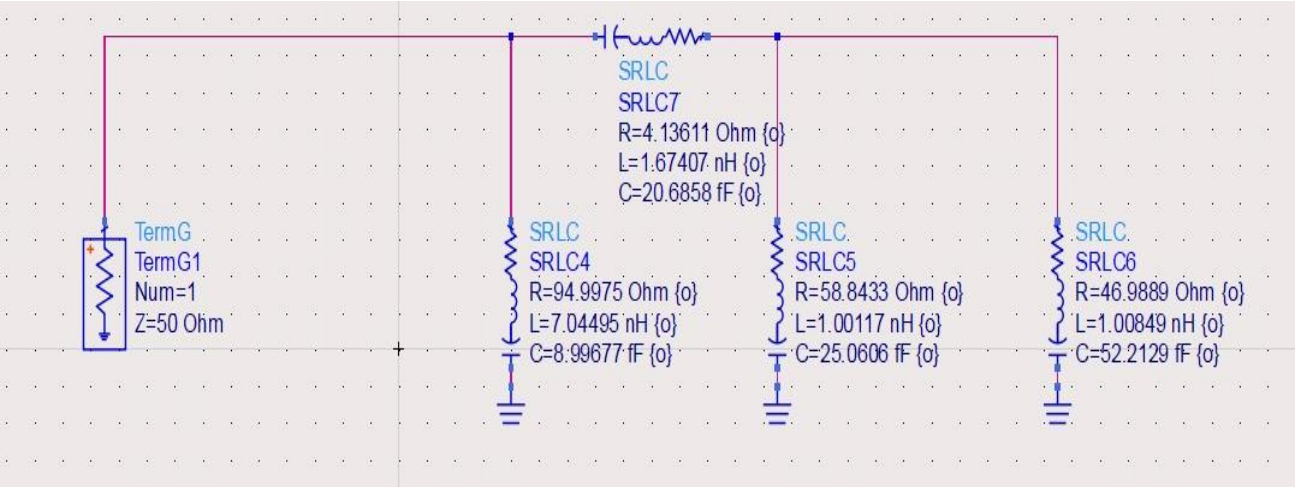


*Figure 41: First design Equivalent circuit model*

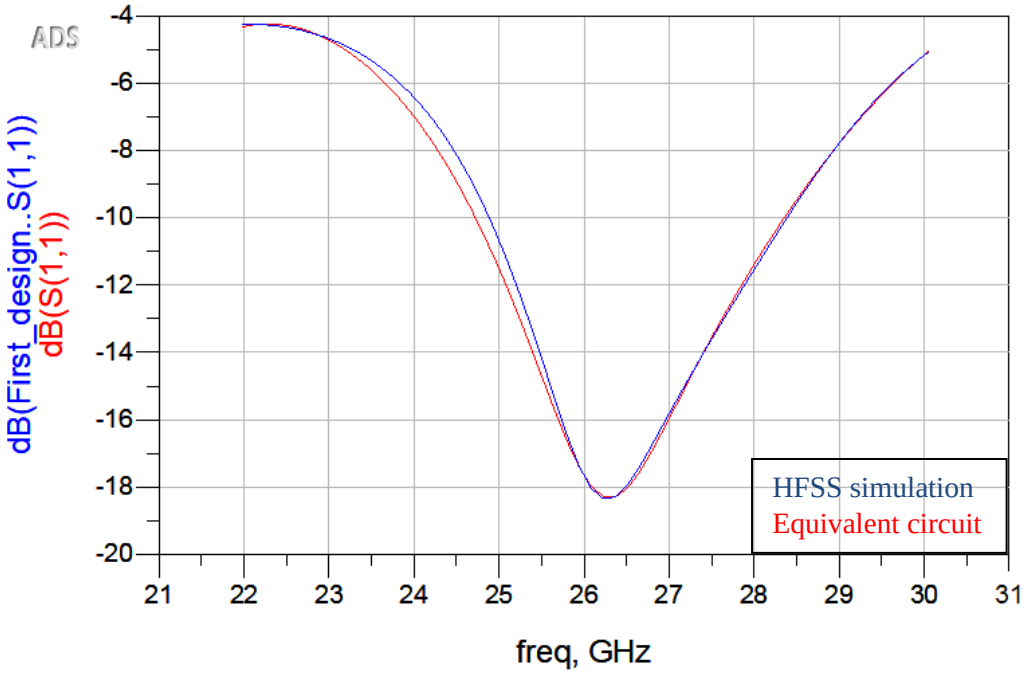


*Figure 42: First design Return loss (dB) of both equivalent circuit model and original structure*

## B. Second Design

We started the operation of getting the model by a few number of parameters but to get accurate results and easy use of the optimizer, we increased the number of parameters to get more degrees of freedom for the simulator to optimize. (observing three notch in design was a good indicator for 3 series filters, and knowing an approximate quality factor from graph and the operating frequency and using these 2 equations $Q = \frac{1}{R}\sqrt{\frac{L}{C}}$ and $f_o = \frac{1}{2\pi\sqrt{LC}}$ to get a good range for L and C for the optimizer to work on. The final equivalent circuit is shown in **figure 43**.

The reflection coefficient **(S11)** calculated from the optimized circuit model was overlaid with the EM simulation results, showing a high degree of alignment, particularly at **26 GHz** as shown in **figure 44**.

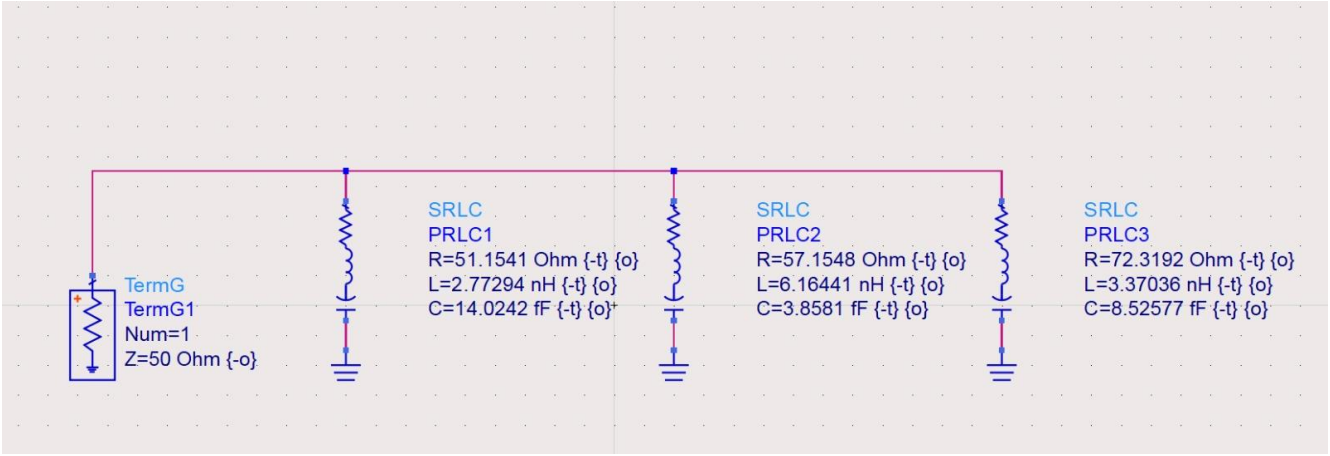


*Figure 43: Second design Equivalent circuit model*

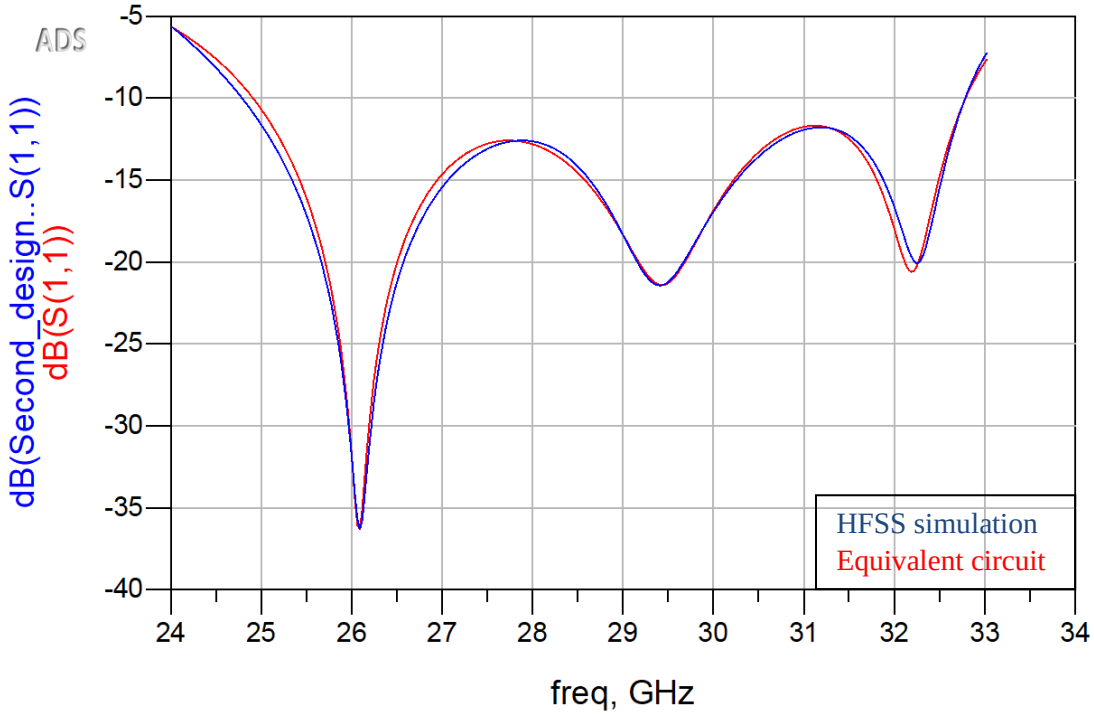


*Figure 44: Second design Return loss (dB) of both equivalent circuit model and original structure*

## 4.8. Effect of spacing between antenna array elements

This section studies the spacing between the antenna array elements and how it effects the antenna parameters for both designs.

This study went through three aspects:

1. Gain
2. Mutual Coupling
3. Active Return Loss

### A. First Design

#### 1. Effect On Gain

Through the **Optimetric** tool provided by HFSS, we could define the spacing between the two elements as a parameter and perform parametric sweep in order to study this effect, which showed strange effects that weren't clearly understandable as shown in **figure 45** with the knowledge that the spacing between the center of two elements in our design is **0.95$\lambda$**.

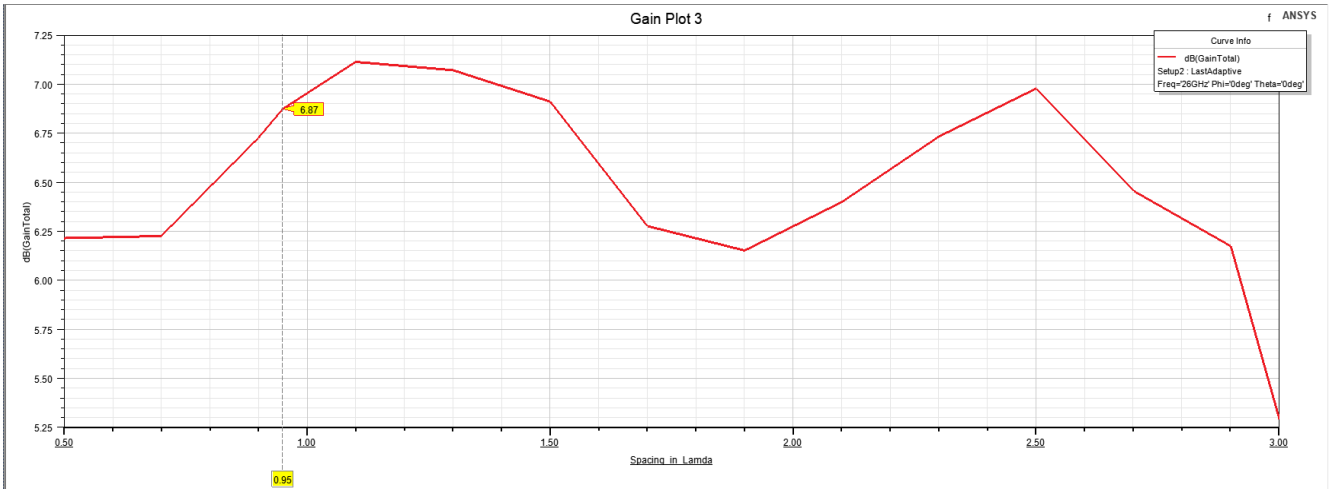


*Figure 45: First design Gain (dB) vs Elements spacing*

## 2. Effect on mutual coupling

We studied the effect of spacing between the antenna array elements through changing the design structure to define two matched ports, one for each antenna as shown in **figures 46 &47**.

Also using **Optimetric,** we could study the effect on the mutual coupling which really makes sense that is as increasing the spacing between the antennas, the mutual coupling decreases gradually as shown in **figure 48**, the mutual couplong in our design is **-55.8 dB**.

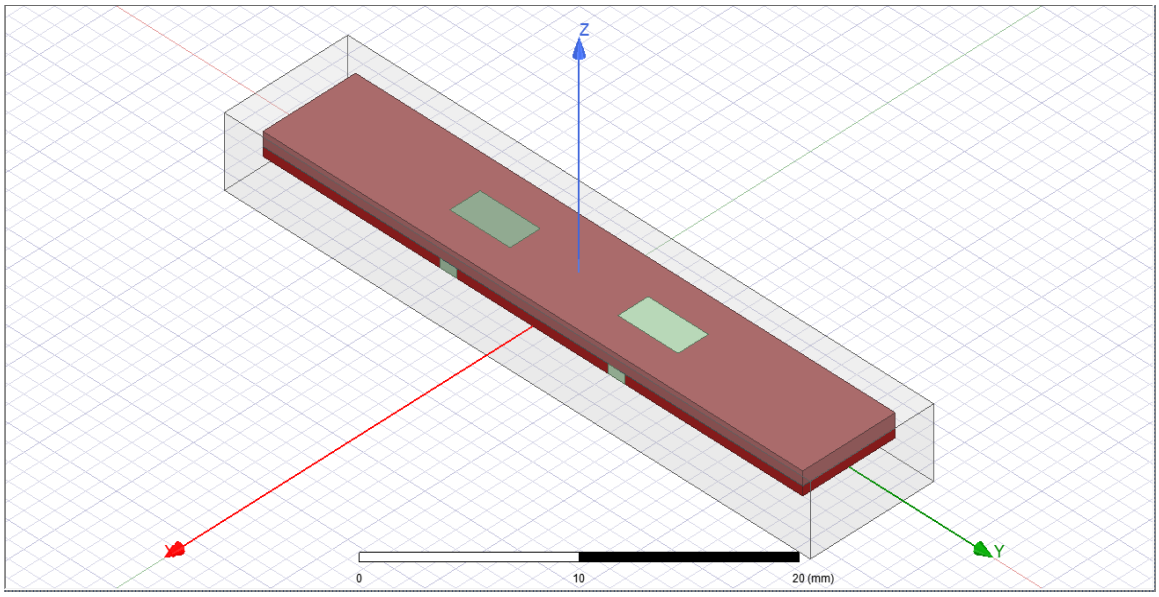


*Figure 46: First design Isometric of reconstructed design to simulate mutual coupling and active return loss*


*Figure 47: First design Bottom side of reconstructed design showing the feeding microstrip line*

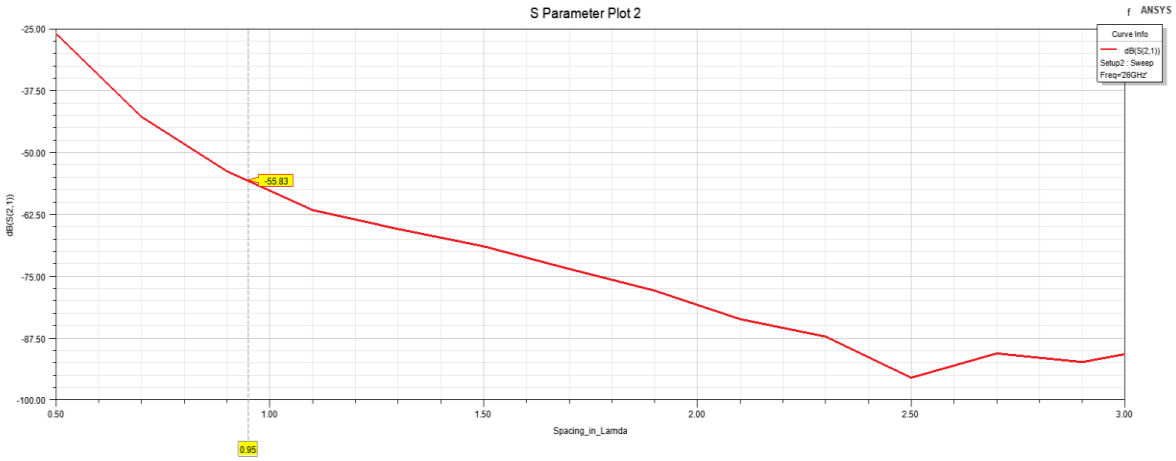


*Figure 48: First design Mutual coupling (dB) vs Elements spacing*

## 3. Effect on Active Return Loss

Results showed almost constant active return loss in range of **0.5$\lambda$** to **2.5$\lambda$** while it starts noticeably increase starting from spacing of **2.7$\lambda$** as shown in **figure 49**.

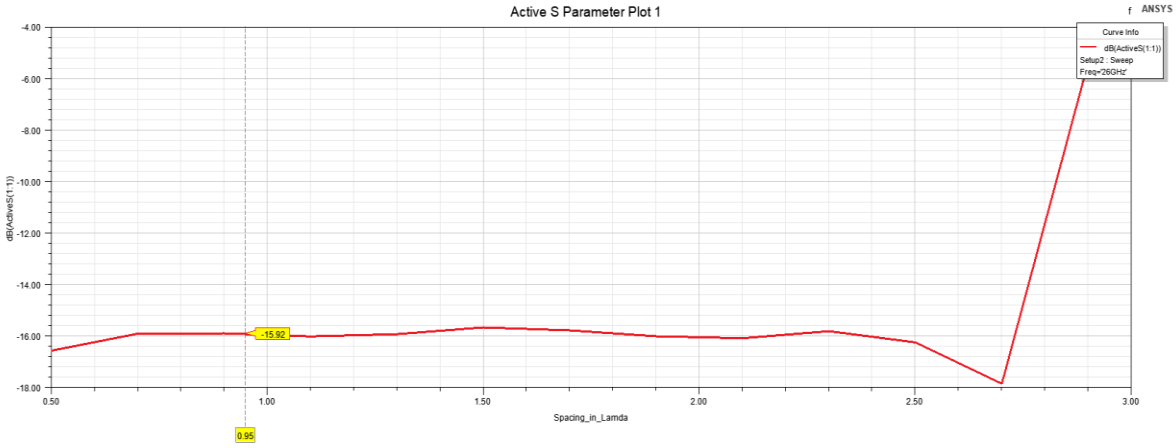


*Figure 49 : First design Active return loss (dB) vs Elements spacing*

## B. Second design

### 1. Effect On Gain

In this design Gain with spacing is not as the previous as the phase because of the feeding network changes so it is divided into two cases without the Feeding network and with it

a) Without the feeding network

Here as the spacing increases, the area increases making enhancing the gain until side lobe introduced that take some power from the main lobe as shown in **figure 50**.

As in the space factor $SF = \left|\frac{\sin\left(\frac{NKd}{2}u\right)}{N\sin\left(\frac{Kd}{2}u\right)}\right|$ meaning when increasing d this compresses the function. So, the radiation pattern has more side lobes in the visible range.

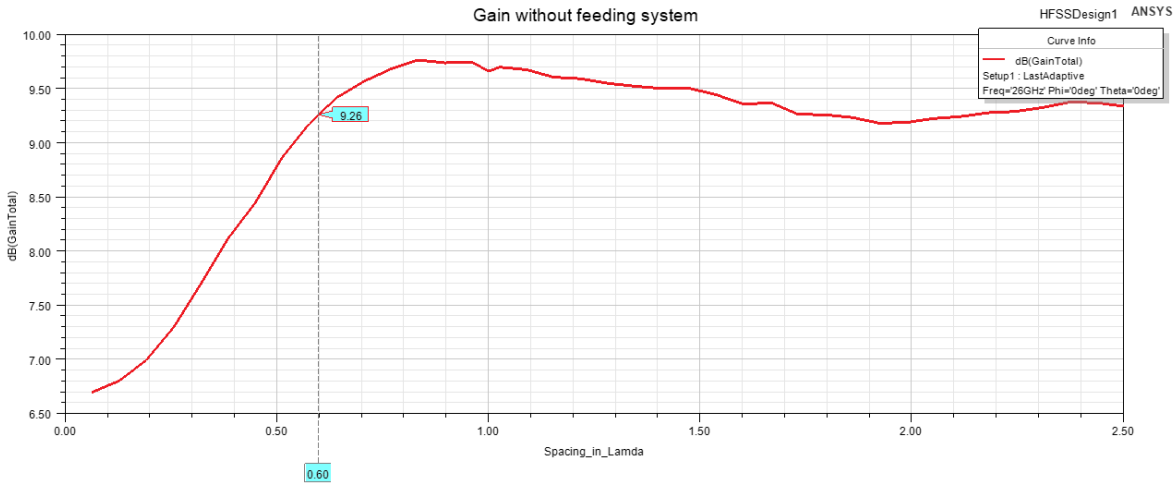


*Figure 50: Second design Gain (dB) vs Elements spacing without the feeding network*

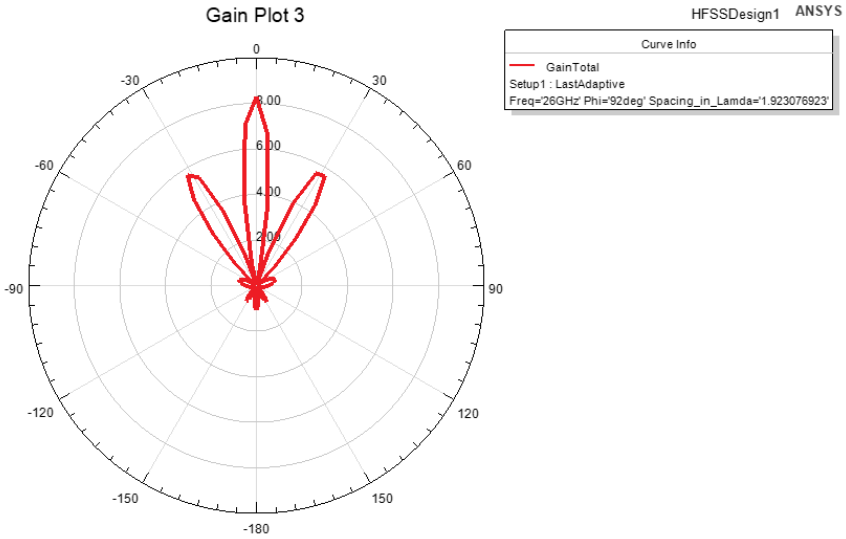


*Figure 51: Second design Radiation pattern (linear) at high elements spacing without the feeding network*

b) With the feeding network

This time we are going to put the feeding network. there is a phase causing two effects.

The gain goes to zero at the intended direction because the main beam tilts as a result of the phase difference between the two elements.

As we see in the space factor equation here $SF = \left|\frac{\sin\left(\frac{NKd}{2}(u-u_{\theta_o})\right)}{N\sin\left(\frac{Kd}{2}(u-u_{\theta_o})\right)}\right|$ here both $u_{\theta_o}$ and d changes

This dual change makes the main beam have side lobes and changes its direction at the same time. We can see the results in **figures 52 &53**.

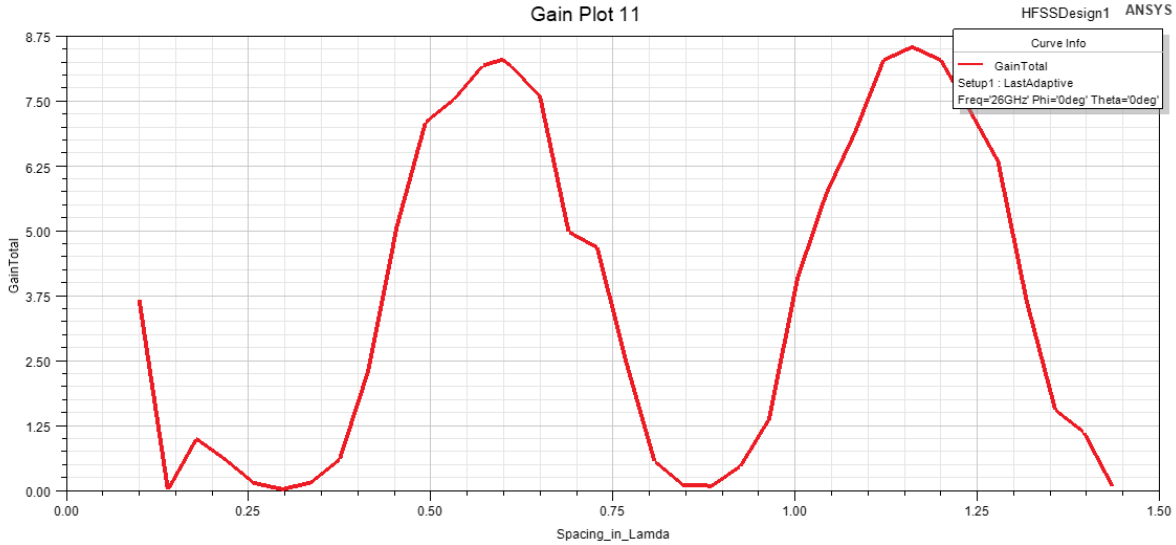


*Figure 52: Second design Gain (dB) vs Elements spacing with the feeding network*

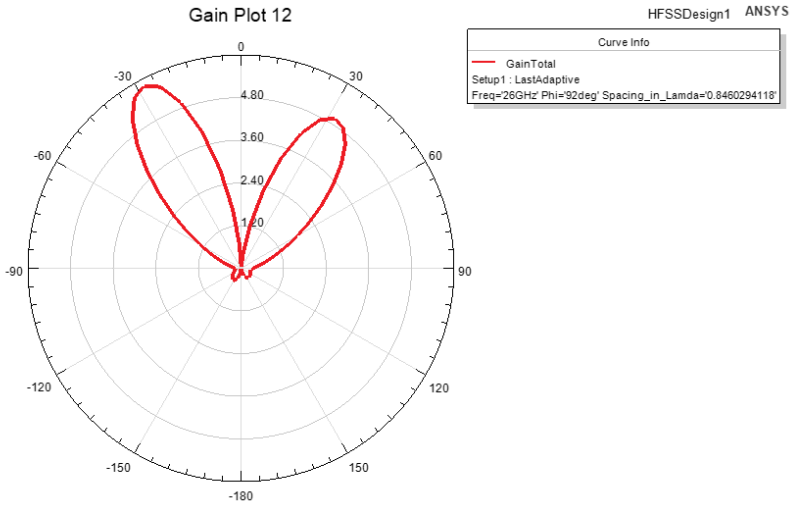


*Figure 53: Second design Radiation pattern (linear) at high element spacing with the feeding network*

Note that original design has spacing of $0.598\lambda$.

## 2. Effect on mutual coupling

We studied the effect of spacing between the antenna array elements through changing the design structure to define two matched ports, one for each antenna as shown in **figures 54 &55**.

Also, through using **Optimetric,** we could study the effect on the mutual coupling which really makes sense that is as increasing the spacing between the antennas, the mutual coupling decreases gradually as shown in **figure**

**56**, the mutual coupling in our design is **-25 dB**. **Figure 57** shows the mutual coupling vs elements spacing at different frequencies in the BW, and **figure 58** shows the mutual coupling vs frequency at different elements spacing.

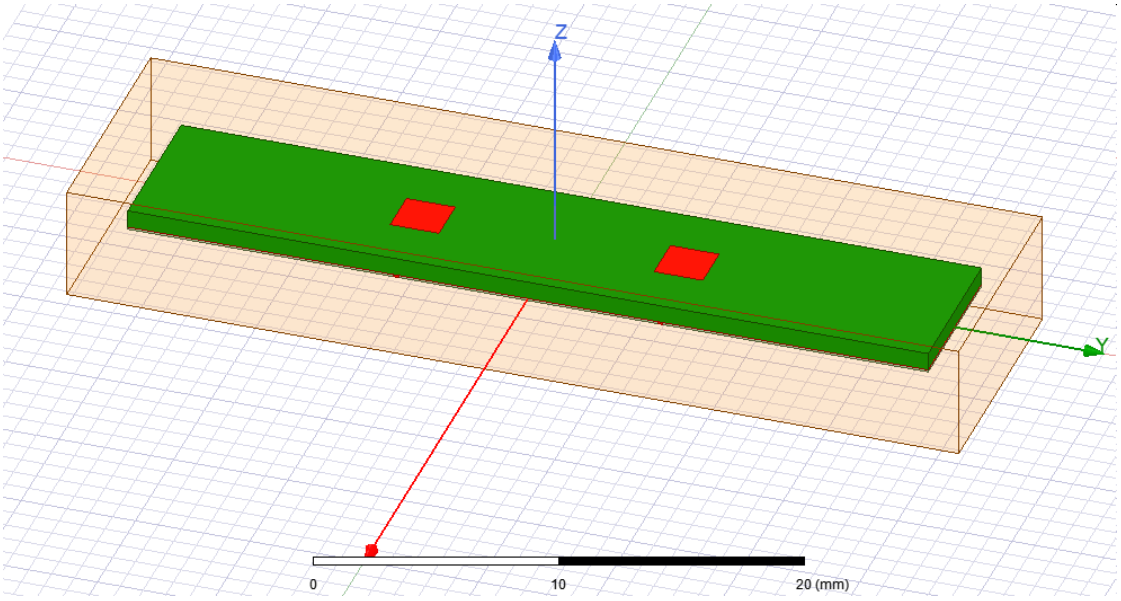


*Figure 54: Second design Isometric of reconstructed design to simulate mutual coupling and active return loss*

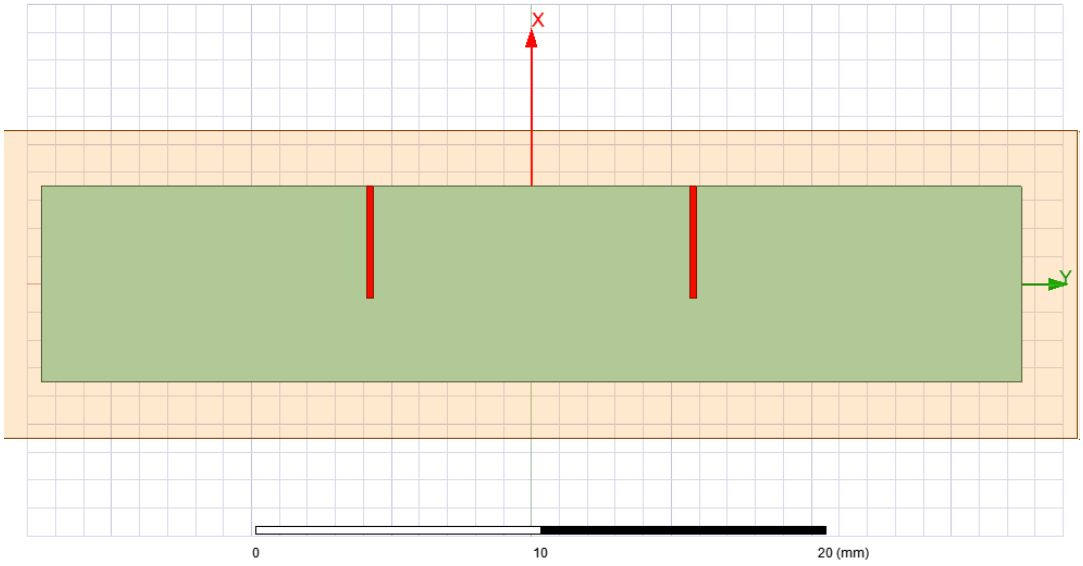


*Figure 55: Second design Bottom side of reconstructed design showing the feeding microstrip line*

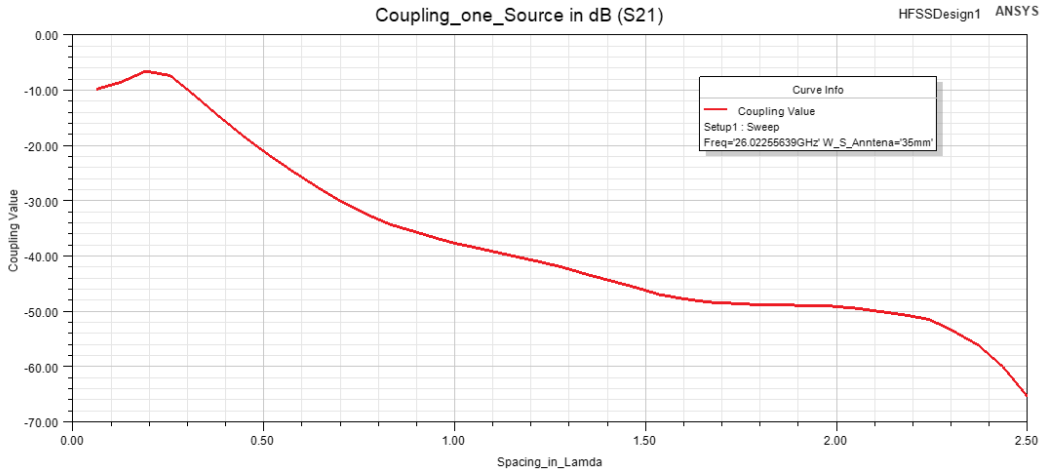


*Figure 56: Second design Mutual coupling (dB) vs Elements spacing*

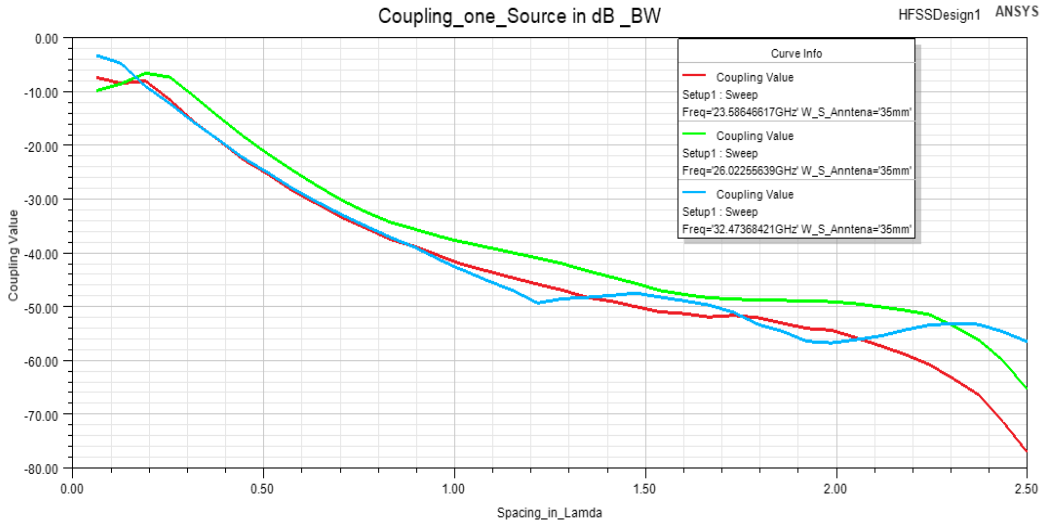


*Figure 57: Second design Mutual coupling (dB) vs Elements spacing at different frequencies in the BW*

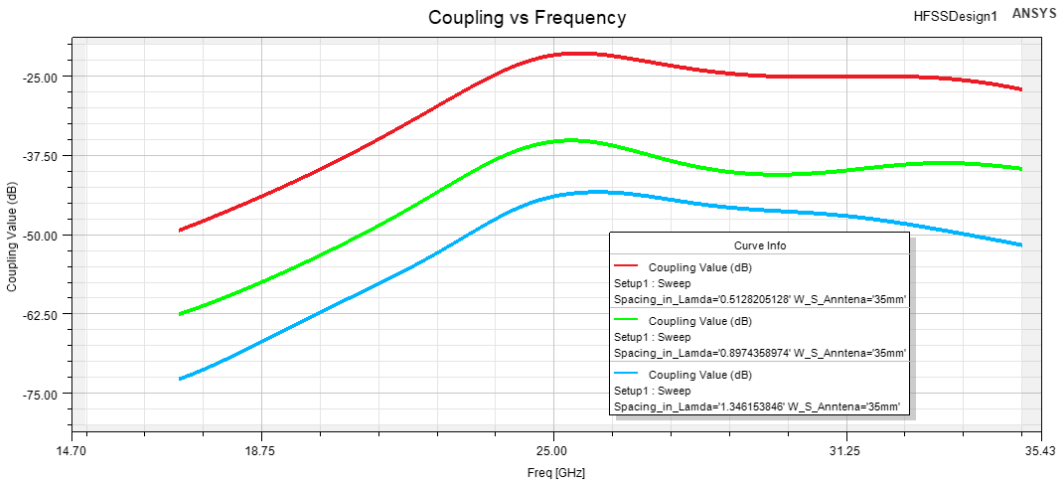


*Figure 58: Second design Mutual coupling (dB) vs frequency at different elements spacing*

### 3. Effect on Active Return Loss

Results showed almost constant active return loss in the range of **0.1$\lambda$** to **2.5$\lambda$** as shown in **figure 59**.

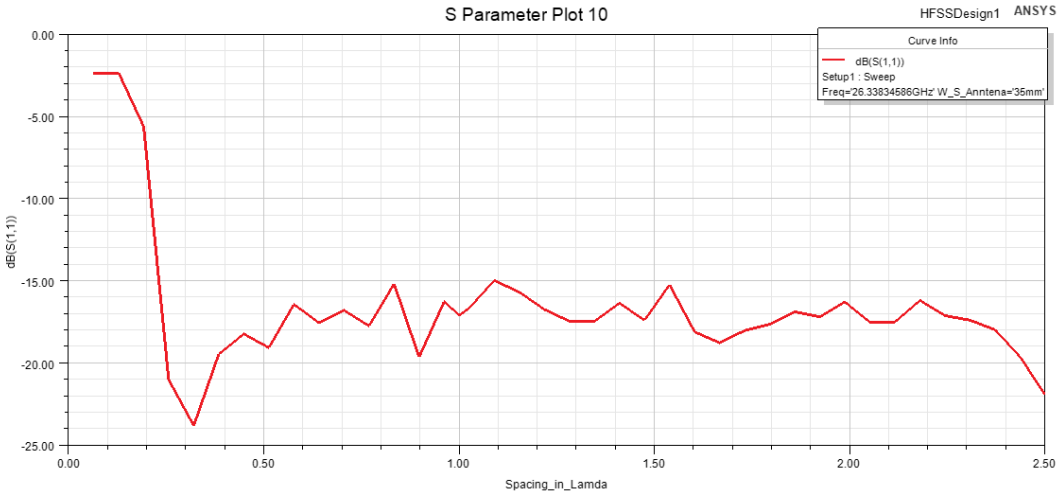


*Figure 59: Second design Active return loss (dB) vs spacing between the two elements for first design*

# 5. Final Design Layout

In this section, we will show our final design layouts for both designs.

The design layout is divided into:

1. Substrates thicknesses and dimensions
2. Patch dimensions and elements spacing
3. Slot dimensions
4. Feeding network

## A. First design

### 1. Substrates thicknesses and dimensions

The material used for the substrates is **Rogers RO4350B**[3], the feed substrate (lower) is **0.508 mm** thickness and the patch substrate is **0.78 mm** thickness, and both are **6 mm** length and **35 mm** width.

### 2. patch dimensions

The patch dimensions are **1.96 mm** length and **3.9 mm** width, The two elements alignment is parallel to their widths (y-axis). As shown in **figure 60**.

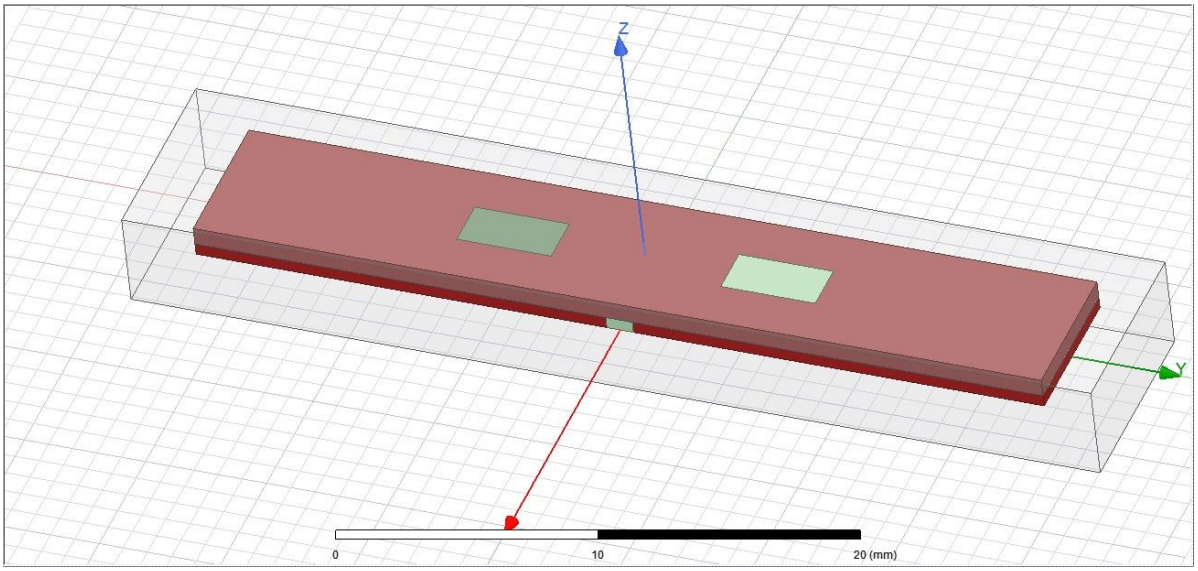


*Figure 60: First design Upper side layout*

### 3. Slot dimensions

The slot is **0.3 mm** length and **2.4 mm** width, where the slot is the same orientation as the antenna as shown in **figure 61**.

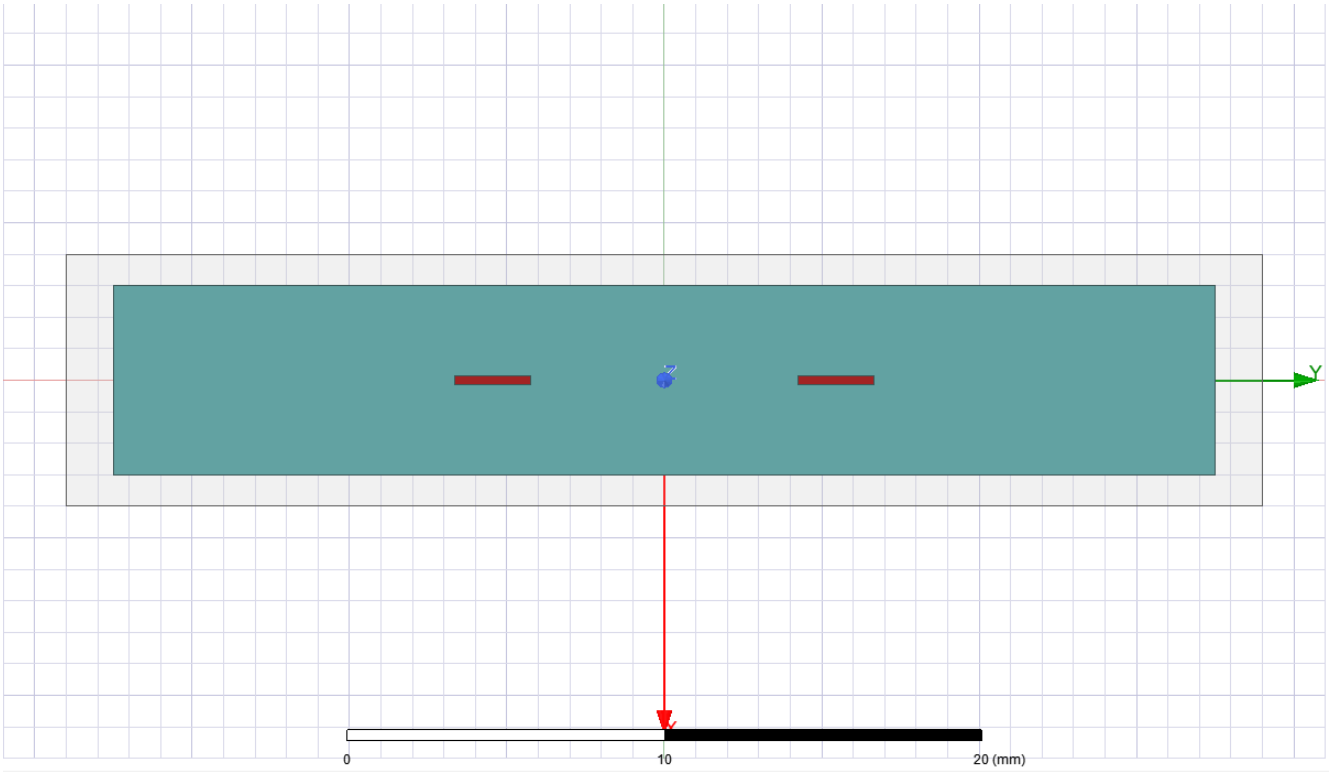


*Figure 61: First design Slot layout*

### 4. Feeding network

The feeding network dimensions are as follows:

1. 50 Ω line width = **1.112 mm**.

2. 70.7 Ω line of width **0.605 mm** and length **1.508 mm**.
3. 100 Ω line of width **0.278 mm**.
   All shown in **figure 62.**

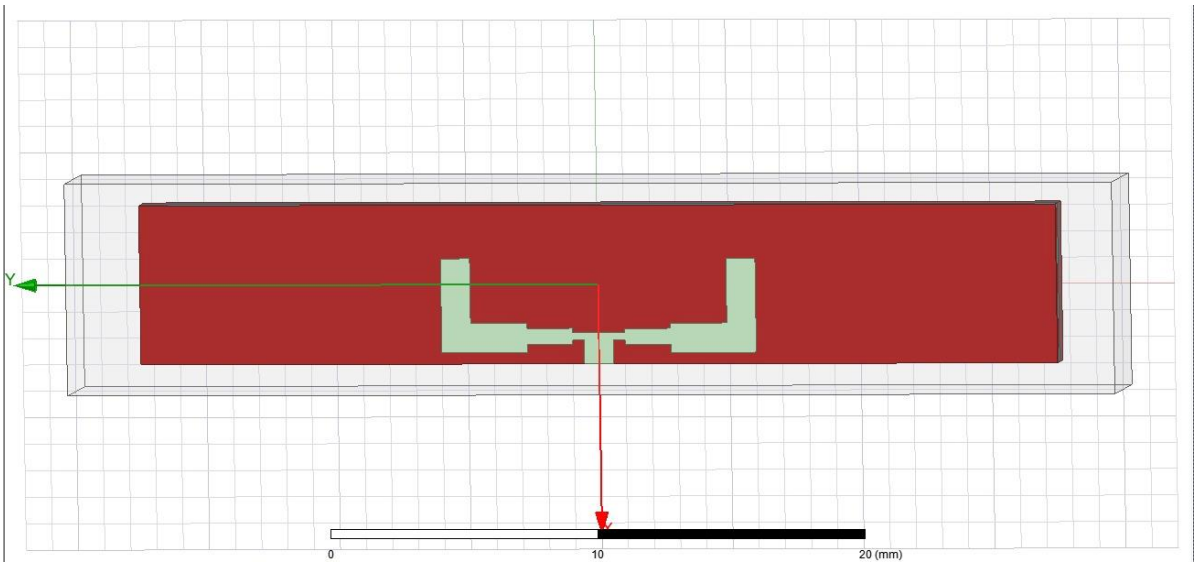


*Figure 62: First design Lower side layout*

# B. Second design

## 1. Substrates thicknesses and dimensions

The material used for the substrates is **Isola TerraGreen (R)**, the feed substrate (lower) is **0.1mm** thickness and the patch substrate is **0.8 mm** thickness, and both are **9 mm** length and **20 mm** width.

## 2. patch dimensions

The patch dimensions are **2.133 mm** length and **2.133 mm** width, The two elements alignment is parallel to their widths (y-axis). As shown in **figure 63**.

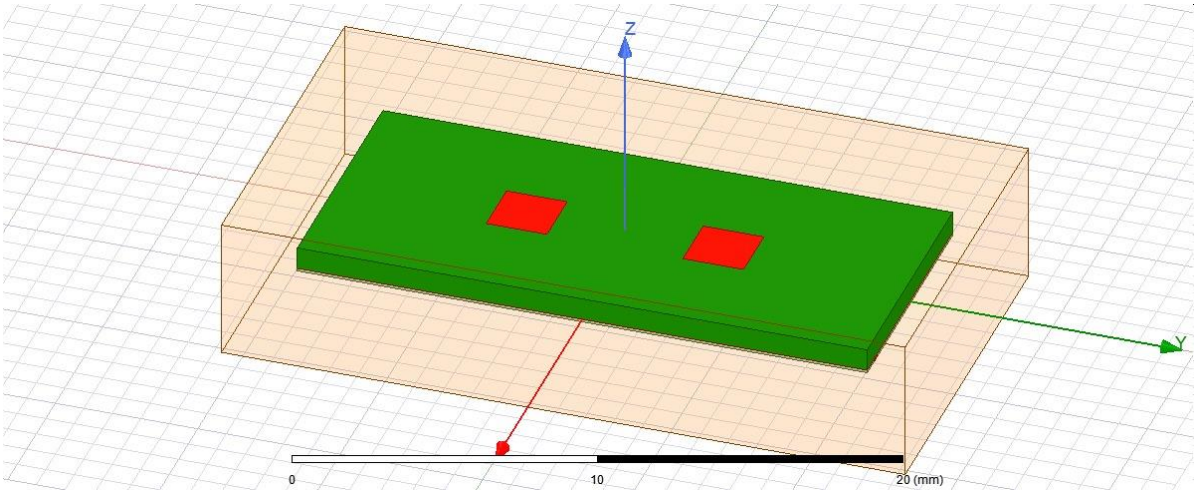


*Figure 63: Second design Upper side layout*

### 3. Slot dimensions

The slot is **0.15 mm** length and **2.019 mm** width, where the slot is the same orientation as the antenna as shown in **figure 64**.

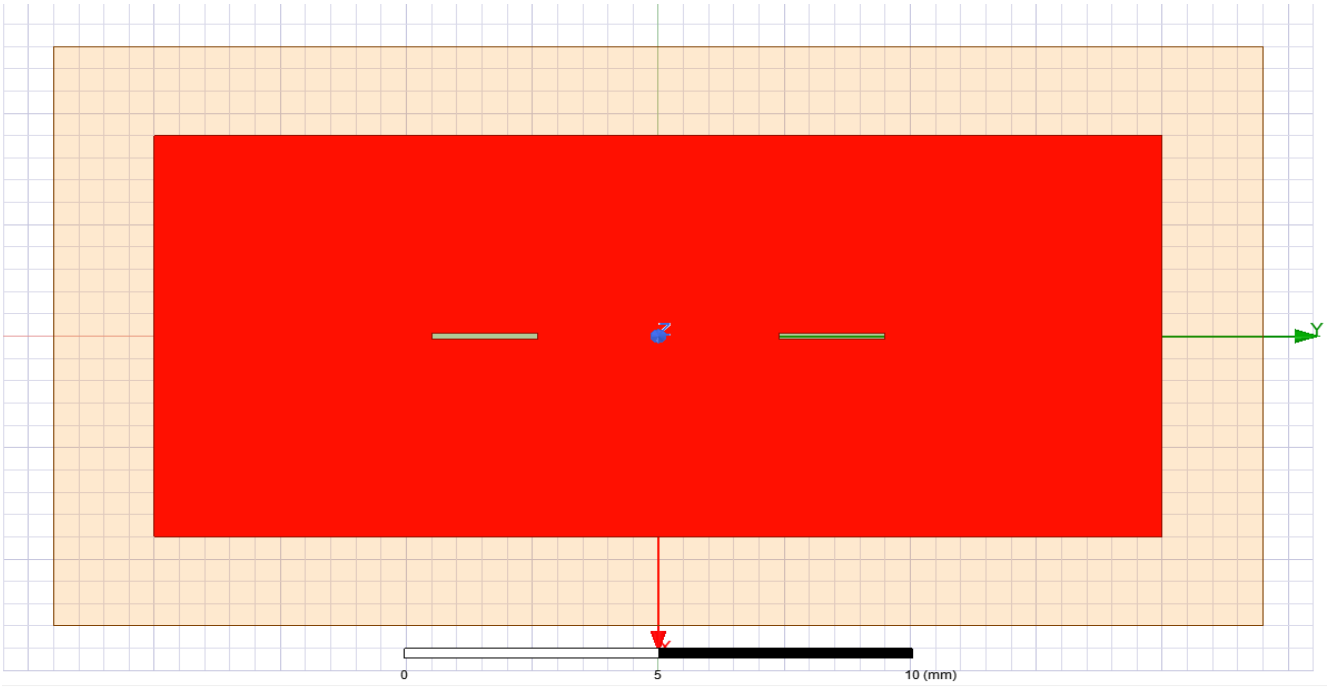


*Figure 64: Second design Slot layout*

### 4. Feeding network

The feeding network dimensions are as follows:

1. 50 Ω line of width **0.22 mm**.
2. 35.35 Ω line of width **0.391 mm** and length **1.6 mm**.
   All shown in **figure 65.**


*Figure 65: First design Lower side layout*

# 6. Conclusion and Future work

This project successfully demonstrates the design, optimization, and analysis of a 2-element slot-fed microstrip patch antenna array for operation at 26 GHz, addressing the critical requirements of next-generation communication technologies like 5G. Two distinct designs were explored, each optimized for specific performance metrics, offering unique strengths to meet diverse application needs.

The first design excels in polarization purity, achieving an axial ratio of **53.69 dB**, and demonstrates better mutual coupling **(-55.8 dB)** and radiation efficiency **(95%)**. These attributes make it ideal for applications prioritizing linear polarization and efficient operation. On the other hand, the second design outperforms in key parameters such as gain **(9.16 dB)**, return loss **(-31.75 dB)**, front-to-back ratio **(10.66 dB)**, and side-lobe suppression **(22 dB)**, making it more suitable for high-gain and dense communication environments. The first design achieved better xz-plane 3-dB beamwidth of **95 degrees**, while the second design achieved better yz-plane 3-dB beamwidth of **44 degrees**. Both designs achieve a relative bandwidth of **13.46%** and maintain stable performance across varying operating conditions, as validated by simulation results.

The study also explored the effects of the spacing between antenna array elements, focusing on gain, mutual coupling, and active return loss. While both designs follow the expected trends, the second design demonstrated more complex behavior due to its feeding network which causes phase difference between the elements.

This study underscores the importance of balancing design trade-offs to achieve specific performance goals in advanced antenna systems. It also highlights the potential of slot-fed microstrip patch arrays to address challenges such as high data rates, low latency, and reliable connectivity.

Looking ahead, future work could focus on scaling the array for higher performance, incorporating active beam-steering technologies, or exploring alternative feeding techniques to improve front-to-back ratios and enhance radiation efficiency. These findings contribute to the broader field of antenna technology, providing a scalable and versatile solution for next-generation wireless networks and paving the way for further research into multi-element arrays and hybrid feeding methods.

*Table 1: Parameters comparison between both designs*

| Antenna parameters | First design | Second design |
|---|---|---|
| **Return loss at 26 GHz (dB)** | -17.65 dB | -31.75 dB |
| **3-dB relative matching Bandwidth** | 13.46% | 30.5% |
| **Input impedance at 26 GHz** | 63.35 – j7 Ω | 48.445 – j1.69 Ω |
| **Gain at 26 GHz (dB)** | 6.9 dB | 9.16 dB |
| **Gain at 26 GHz (linear)** | 4.95 | 8.24 |
| **Front-to-back ratio (dB)** | 6.9 dB | 10.66 dB |
| **Side-lobe level (dB)** | 8.5 dB | 22 dB |
| **xz-plane Beamwidth** | 95° | 76° |
| **yz-plane Beamwidth** | 28.7° | 43.76° |
| **Axial ratio at 26 GHz (dB)** | 53.69 dB | 38.73 dB |
| **1-dB relative gain Bandwidth** | 15.18% | 14.6% |
| **Intersected operating relative Bandwidth** | 13.46% | 13.46% |
| **Mutual coupling (dB)** | -55.8 dB | -25 dB |

# 7. References


1. E. Setijadi, "Gain Enhanced 26 GHz Antenna for 5G Communication Technology," *Progress In Electromagnetics Research C*, vol. 139, pp. 187-195, Dec. 2023.
2. C. Seker and M. T. Güneşer, "Design and simulation of 26 GHz patch antenna for 5G mobile handset," *2019 11th International Conference on Electrical and Electronics Engineering (ELECO)*, Bursa, Turkey, 2019, pp. 1060-1064.
3. Rogers Corporation, *RO4000 Series High Frequency Circuit Materials*. Advanced Connectivity Solutions, Chandler, AZ, USA, 2018.
4. E. A. Soliman, A. Vasylchenko, V. Volski, G. A. E. Vandenbosch, and W. De Raedt, "Series-Fed Microstrip Antenna Arrays Operating at 26 GHz," presented at the IEEE Antennas and Propagation Society International Symposium (APS), 2010.
5. D. Nashaat, H. A. Elsadek, and E. A. Abdallah, "Design of Microstrip Antenna for WLAN," *Progress In Electromagnetics Research C*, vol. 3, pp. 219–226, 2008.
6. A. Al-Zoubi, A. Al-Hunaity, H. Al-Khateeb, and S. Safouti, "Design and Performance of Resonant Spacing Linear Patch Array with Mitered Bend Feed Network for Wireless Applications," *International Journal of Microwave and Wireless Technologies*, vol. 9, no. 1, pp. 1–9, 2017.